X-321-67-634

NASA TM X-63128

FLIGHT VIBRATION DATA OF ASTROBEE 1500, NASA FLIGHT 16.02

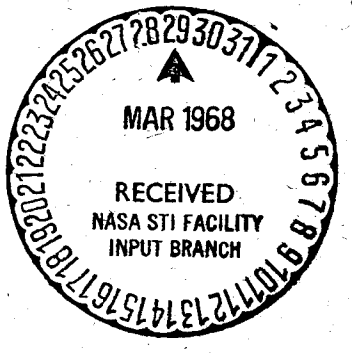

GPO PRICE $ _____

CFSTI PRICE(S) $ _____

Hard copy (HC) 3.00

Microfiche (MF) .65

DECEMBER 1967

ff 653 July 65

GSFC

GODDARD SPACE FLIGHT CENTER

GREENBELT, MARYLAND

X-321-67-634

FLIGHT VIBRATION DATA OF ASTROBEE 1500, NASA FLIGHT 16.02

Arney N. Munson
Test and Evaluation Division
Systems Reliability Directorate

December 1967

GODDARD SPACE FLIGHT CENTER
Greenbelt, Maryland

FLIGHT VIBRATION DATA OF ASTROBEE 1500, NASA FLIGHT 16.02

Prepared by: Arney N. Munson
Arney N. Munson
Structural Research and Technology Section

Reviewed by: J. P. Young
J. P. Young
Head, Structural Research and Technology Section

E. J. Kirchman
E. J. Kirchman
Head, Structural Dynamics Branch

Approved by: John H. Boeckel
John H. Boeckel
Associate Chief, Test and Evaluation Division

PROGRAM STATUS

This is the final report on the vibration data obtained from the Astrobee 1500, NASA Flight 16.02.

Authorization
Test and Evaluation Division charge number: 321-124-08-05-03

FLIGHT VIBRATION DATA OF ASTROBEE 1500, NASA FLIGHT 16.02

Arney N. Munson
Goddard Space Flight Center

SUMMARY

This report presents payload vibration data obtained during the launch of the two-stage Astrobee 1500 sounding rocket. Three channels of high-frequency vibration data were obtained from crystal accelerometers mounted on the payload support structure. High vibratory transient response levels were noted at first- and second-stage ignition and just after first-stage burnout. The former responses are typical of rocket engine ignition; however, the latter response is attributed to the anomalous release of the clam-shell heat shield.

Relatively low level random responses, less than 1 g rms, were noted during the flight periods of transonic, maximum dynamic pressure, and shortly after second stage burnout. Also measured were rigid body coning motions that occurred at about T+98 seconds, 20 seconds after second stage burnout. This motion is thought to have been initiated by the unwrapping of the spun fiberglass motor case caused by high motor temperatures.

CONTENTS

TABLES

ILLUSTRATIONS

ILLUSTRATIONS (Continued)

ILLUSTRATIONS (Continued)

FLIGHT VIBRATION DATA OF ASTROBEE 1500, NASA FLIGHT 16.02

Arney N. Munson
Goddard Space Flight Center

INTRODUCTION

This report presents the flight vibration data obtained from the Astrobee 1500 Launch, NASA 16.02. The vehicle was launched on October 21, 1964 from NASA Wallops Station, Wallops Island, Virginia.

The primary objective of NASA flight number 16.02 was to verify certain design changes incorporated in the vehicle as a result of previous Astrobee failures and to determine the flight performance of the vehicle in order to assess its usefulness in the National Sounding Rocket Program. A secondary objective of 16.02 was to define the vibration environment imposed on the payload in order to develop payload design and vibration testing criteria.

The purpose of this report is to present only the flight vibration data of the payload and not to evaluate the total performance of the vehicle.

PAST HISTORY

The firing of the 16.02 constitutes the fifth flight of the Astrobee 1500 sounding rocket vehicle. This vehicle was developed as a company-funded project by Space-General Corporation, El Monte, California. The first two Astrobees were fired from the Naval Missile Test Facility at Point Arguello, California as joint projects of Space General and the Air Force Cambridge Research Laboratories. The third shot, also from Point Arguello, was conducted by the Sandia Corporation. The second firing only resulted in a satisfactory flight; the first and third failing at T+22.6 and T+16.5 seconds respectively due to structural failure of the vehicle. Data from the second launch was lost after T+52 seconds due to loss of telemetry.

The fourth Astrobee 1500 vehicle, designated NASA 16.01, was acquired by NASA from Sandia Corporation by means of a trade for an Argo D-4 Rocket. This vehicle incorporated structural modifications dictated by previous structural failures. The 16.01 was launched from Wallops Island on April 8, 1963, however it too resulted in structural failure of the vehicle. Examination of photographic records and other evidence disclosed that this vehicle and the

previous failures were due to marginal design of the clamshell heat shields which ruptured under pressure buildups encountered during flight.

VEHICLE DESCRIPTION

The Astrobee 1500 is a two stage, solid propellant high performance sounding rocket designed to carry a 100 lb. payload to an apogee of about 1500 miles. Figure 1 shows a picture of 16.02 as it cleared its launcher at Wallops Station. The first stage is a four-finned Aerojet Junior and is assisted by two solid propellant auxiliary "Recruit" boosters. The second stage is an Aerojet 30 KS 8000 "Alcor" rocket which utilizes conical flare plus minimal spin for near neutral aerodynamic stability. Four 1 KS-210 motors are used to spin up the second stage before firing. First stage burning time is 40 seconds. The second stage burns for 30 seconds. The Recruit boosters are retained after their nominal 2.4 second burn time. Figure 2 is a view of Astrobee 16.02 on its tubular launcher at Wallops Station, Virginia, and indicates its component parts.

Vehicle weight without payload was 11,500 lb. Second stage payload weight was 133.7 lb. An additional first stage telemetry package, termed the interstage payload, weighed an additional 22 lb., bringing the total payload weight to 155.7 lb. Normal apogee with this payload weight is 1142 miles.

DESCRIPTION OF EXPERIMENT

The second stage payload can be seen in Figure 3 before assembly onto the rocket. The payload consisted of the second stage flight instrumentation, mounting hardware, and telemeter. The second smaller payload, located in the interstage, carried the first stage instrumentation and telemeter.

The vibration experiment was located within the second stage payload and consisted of longitudinal, pitch, and yaw vibration channels. The transducers were of the piezoelectric type, each with a flat frequency response from 20 Hz to above 5 kc, and were located at the base of the payload mount ring as depicted in Figure 4.

A diagram of the flight vibration system is shown in Figure 5. Accelerometer signals were amplified by charge amplifiers; the inputs to these amplifiers were frequency low passed to limit the channels to their respective IRIG frequency allocations. The signals then modulated their respective voltage controlled oscillators, were mixed to form the subcarrier, and were transmitted.

The frequency response of each of the three vibration channels after low-pass filtering is shown in Figure 6.

DATA REDUCTION SYSTEM

A simplified functional diagram of the data reduction procedure used for the 16.02 data is shown in Figure 10. The frequency modulated (FM) subcarrier signal is fed into discriminators, which restore the data to the analog form. From this analog signal, composite records, narrow band filtered records, and RMS level records are produced. Probability density and power spectral density analyses are performed during those portions of the flight where the data becomes predominently random.

Frequency responses and amplitude linearity responses of the total instrumentation system for each channel are shown in Figures 8 and 9. These responses are total system responses and relate an input g level experienced by a transducer to the output signal from the readout of the data reduction system in the laboratory.

During those portions of the flight where shock-excited transient responses were observed, a narrow band oscillograph was obtained in order to determine the vibratory acceleration level. Roll-off of the filters utilized was 24 decibels (db) per octave beyond the 3 db points. The 3 db-down points and the filter center frequency are noted on each record. An acceleration scale in ±g, 0-peak is presented with each record in order that the reader may determine the acceleration levels of any portion of the record at will. A composite acceleration trace is included on each record for comparison with the filtered traces. Periods during which the telemeter signal was lost and "ringing" of the filter caused by these signal losses are indicated by an asterisk (*). These periods do not constitute valid data and are to be disregarded.

RESULTS OF DATA ANALYSIS

Vehicle performance is summarized below for reference purposes. A typical vs actual sequence of events for the flight is presented in Table 1. As can be observed from this table, all events occurred slightly prematurely.

Vehicle altitude and vehicle velocity vs flight time are presented in Figures 10 and 11 respectively. The maximum altitude which the vehicle reached was 1190 statute miles at time T+14.2 minutes. The maximum first stage velocity achieved was 6.2×10^3 feet/second and maximum second stage velocity was 17.42×10^3 feet/second.

Table 1
Typical vs Actual Sequence of Events for NASA Flight 16.02

Programmed Event Time	Actual Time Event Observed	Events
T + 0	0 sec	First-stage junior ignition.
T + 2.4 sec	1.9 sec	Two Recruits burned out and remained attached to first stage.
T + 40.1 sec	37.5 sec	First-stage junior burned out and remained attached to second stage.
Anomaly	38.4 sec	Clamshell heat shield opened and dropped off without being released.
T + 48 sec	45.2 sec	Four 1 KS-200 motors, mounted within the interstage assembly, fired and spun up the second stage and payload to 10 rps. Rotation released explosive bolt timer.
T + 49.5 sec		Clamshell heat shield was programmed to open.
T + 50 sec	47.4 sec	Second-stage Alcor ignited and blast separated the first stage.
T + 80 sec	74.0 sec	Second-stage Alcor burned out and remained with payload.
Anomaly	104 sec	Insulation wrap from second-stage motor unwrapped causing erratic vehicle motion and decrease of spin to near zero, thus compromising the two despin experiments.
T + 10 min		Squib-actuated pin pullers were programmed to release first yo-yo despin system. Payload was to despin from 12.5 to 9 rps.
T + 15 min		Squib-actuated pin pullers were programmed to release second yo-yo despin. Payload was to despin from 9 to 6 rps.
T + 16 min, 15 sec	14 min, 6 sec	Apogee
T + 31 min, 22 sec	27 min, 52 sec	Splash down

A slow speed analog data record of longitudinal acceleration, plus the three vibration channels, for the entire flight can be seen in Figure 12. Maximum first stage steady state acceleration during recruit burning was 14.1 g; maximum first stage acceleration after recruit burnout was 14.5 g. The maximum steady state acceleration produced during second stage burning was 36.9 g.

Records of vibration level, in g-RMS, vs flight time are presented for the three vibration channels in Figures 13, 14, and 15. It can be seen from these figures that all RMS levels for the flight were below 1 g RMS. These records give a good indication of the energy levels present in the signal, particularly that portion which is random in nature. Transonic and maximum dynamic pressure regions of flight are noted from these records by a large increase in the RMS level during first stage burning. It is in these regions that the nature of the data becomes random due to the high acoustic environment encountered throughout these periods.

For the most part, transient sinusoidal vibrations measured during flight of the Astrobee 1500, NASA 16.02, were relatively low in level. Exceptions were the high levels measured during first and second stage ignition and a high amplitude excitation that occurred during first stage burning at T+38 seconds. This high amplitude excitation is believed to have been caused by the loss of the clamshell heat shields eleven seconds prior to planned release. An over-all summary of the predominant frequencies for the entire flight and their associated maximum levels is presented in Table 2.

First Stage Ignition

Vibration responses for first stage ignition were as indicated in Table 3. Figure numbers of illustrations corresponding to the various responses listed in the following tables, are noted for reference purposes.

As noted in Table 3, 50 Hz longitudinal vibration responses are produced at lift-off while 67 Hz is seen to predominate in both lateral axes. The two lateral axes are seen to exhibit almost identical vibration data.

First Stage Burn

After approximately 30 seconds of first stage burning, transients appeared, and continued until burn-out at T+37 seconds. Vibrations of 11.5 Hz and 75 Hz in pitch and yaw axes are noted during this period. Shortly thereafter, at T+38.4 seconds, an anomalous event occurred which produced very high structural vibration levels. This is believed to have been caused by premature loss of the clamshell heat shield, which dropped off without operation of the release mechanism, eleven seconds prior to planned release. Vibrations produced during these periods were as indicated in Table 4.

Table 2

Vibration Frequencies and Levels for NASA Flight 16.02

	IRIG E Longitudinal Vibration			IRIG C Pitch Vibration			IRIG A Yaw Vibration		
	Time (sec)	Level (g)	Freq. (Hz)	Time (sec)	Level (g)	Freq. (Hz)	Time (sec)	Level (g)	Freq. (Hz)
First-stage burn	0.3	2.71	50	0.3	0.35	67	0.3	0.35	67
	—			0.6	0.12	9.3	0.6	0.10	9.3
	6.7	0.61	50	—			—		
	—			8	0.15	8	8	0.15	8
	16.3	0.67	50	—			—		
	—			31.6	0.40	11.5	31.6	0.65	75
	—			—			31.6	0.54	11.5
	38.4	0.45	12.5	38.4	1.22	12.5	38.4	1.26	12.5
	38.4	3.01	56	38.4	1.99	56	38.4	4.66	56
	38.4	3.22	790	38.4	26.0	1200	38.4	4.80	790
	—			—			38.5	0.83	167
	—			—			38.5	0.96	225
Second-stage burn	45.3	0.36	50	—			—		
	45.3	0.21	8	—			—		
	48	0.36	8	—			—		
	48.8	4.41	300	—			—		
	—			65.4	0.55	200	65.4	0.81	200
	—			66.2	0.52	200	66.2	0.49	200
	—			66.5	0.29	200	66.5	0.29	200
	75	0.20	8	—			—		
	—			86.9	0.42	140	—		
	—			—	—	—	87.4	0.43	225
	—			88	0.22	6.1	88	0.32	6.1
	—			—			90	0.72	225
	98	0.21	8	—			—		
	—			97	1.19	6.2	97	1.79	6.2
	—			97	1.35	140	97	1.15	140
	104.6	7.10	5.1	104.6	2.10	3.3	104.6	2.10	3.3

Table 3

Vibration Data, First-Stage Ignition

Event	Time (sec)	Axis	Level 0 to pk (g)	Frequency (Hz)	Figure
First-stage ignition	0.3	Longitudinal	2.71	50	16
First-stage ignition	0.3	Pitch	0.35	67	17
First-stage ignition	0.3	Yaw	0.35	67	18
First-stage ignition	0.6	Pitch	0.12	9.3	17
First-stage ignition	0.6	Yaw	0.10	9.3	18
Transonic/max Q	6.7	Longitudinal	0.61	50	19
Transonic/max Q	8.0	Pitch	0.15	8.0	-
Transonic/max Q	8.0	Yaw	0.15	8.0	-
Transonic/max Q	16.3	Longitudinal	0.68	50	20

Second Stage Spin-up and Burning

At T+45.2 seconds spin up of the second stage occurred but was greatly obscured by the loss of RF signal. Low-level 50 Hz and 8 Hz vibrations appeared shortly after spin-up. A transient response of unknown origin occurred at T+45.7 seconds producing levels up to 15.7 g. Second stage ignition occurred at T+47.4 seconds and was partly obscured by drop-out of RF signal. Vibration responses for this period are as indicated in Table 5.

An eight cps rigid body response, indicative of coning motion, is seen to increase slowly from 0.21 g after spin-up to 0.36 g after second stage ignition. No lateral vibrations are noted during this period.

Second Stage Burning

Second stage burning transients are seen to be relatively low in level and all produced 200 Hz transient sinusoidal vibrations. No longitudinal vibrations were produced throughout this period. Second stage burn-out was characterized by a series of transients in addition to a period of random data, the analysis of which will be treated in a later section. The low level 8 cps coning acceleration which appeared after spin-up slowly decreased in level to 0.20 g and remained there until T+104 seconds.

Table 4
Vibration Data, First-Stage Burn

Event	Time (sec)	Axis	Level 0 to pk (g)	Frequency (Hz)	Figure
First-stage burn	31.6	Pitch	0.40	11.5	21
First-stage burn	31.6	Yaw	0.65	75	22
First-stage burn	31.6	Yaw	0.54	11.5	22
Loss of heatshield	38.4	Longitudinal	0.45	12.5	23
Loss of heatshield	38.4	Longitudinal	3.01	56	23
Loss of heatshield	38.4	Longitudinal	3.22	790	24
Loss of heatshield	38.4	Pitch	1.22	12.5	25
Loss of heatshield	38.4	Pitch	1.99	56	25
Loss of heatshield	38.4	Pitch	26.0	1200	26
Loss of heatshield	38.4	Yaw	1.26	12.5	27
Loss of heatshield	38.4	Yaw	4.66	56	27
Loss of heatshield	38.4	Yaw	4.80	790	28
Loss of heatshield	38.5	Yaw	0.83	167	-
Loss of heatshield	38.5	Yaw	0.96	225	29

Second Stage Post Burn-Out

After second stage burn-out a series of responses were noted in the two lateral axes. An over-all view of these responses can be observed in Figure 36. These responses are indicative of measuring system overload and recovery and while the response amplitudes do not correspond to actual excitation magnitudes they do indicate the presence of some form of excitation. A series of these overload responses occurred, commencing at T+81 seconds, with a 6 Hz acceleration appearing at T+88 seconds and later intensifying at T+97 seconds. Finally at T+104 seconds, extreme motions of the vehicle occurred accompanied by a change of spin rate from 8.2 revolutions per second to 5.1 revolutions per second, as ascertained from rate gyro records. It is believed that at this point the second stage motor case had failed structurally due to high motor temperatures. A further decrease of spin brought the spin rate down to near zero at T+150 seconds, thus compromising the two yo-yo despin experiments.

Table 5
Vibration Data, Second-Stage Ignition

Event	Time (sec)	Axis	Level 0 to pk (g)	Frequency (Hz)	Figure
Second-stage spinup	45.3	Longitudinal	0.36	50	30
Second-stage spinup	45.3	Longitudinal	0.21	8	30
Unknown response	45.8	Longitudinal	2.80	Impulse (10-2100)	30
Unknown response	45.8	Pitch	15.72	Impulse (10-1200)	31
Unknown response	45.8	Yaw	2.68	Impulse (10-660)	31
Second-stage ignition	47.4	Longitudinal	10.0	Impulse (10-2100)	30
Second-stage ignition	47.4	Pitch	4.22	Impulse (10-1200)	31
Second-stage ignition	47.4	Yaw	7.66	Impulse (10-660)	31
Second-stage ignition	48.0	Longitudinal	0.36	8	30
Unknown event	48.8	Longitudinal	4.41	300	32

Table 6
Vibration Data, Second-Stage Burn

Event	Time (sec)	Axis	Level 0 to pk (g)	Frequency (Hz)	Figure
Second-stage burn	65.4	Pitch	0.54	200	33
Second-stage burn	65.4	Yaw	0.81	200	34
Second-stage burn	66.2	Pitch	0.52	200	33
Second-stage burn	66.2	Yaw	0.49	200	34
Second-stage burn	66.5	Pitch	0.29	200	33
Second-stage burn	66.5	Yaw	0.29	200	34
Coning motion	75.0	Longitudinal	0.20	8	35

Table 7
Vibration Data, Erratic Motion of Vehicle

Time (sec)	Axis	Level 0 to peak (g)	Frequency (Hz)	Figure
86.9	Pitch	0.42	140	-
87.4	Yaw	0.43	225	37
88.0	Pitch	0.22	6.1	-
88.0	Yaw	0.32	6.1	-
90.0	Yaw	0.72	225	38
97.0	Pitch	1.19	6.2	39
97.0	Pitch	1.35	140	40
97.0	Yaw	1.79	6.2	41
97.0	Yaw	1.15	140	42
103.5	Longitudinal	0.20	8	43
104.6	Longitudinal	7.10	5.1	43
104.6	Pitch	2.10	3.3	43
104.6	Yaw	2.10	3.3	43

Random Vibration Data

Flight data of the Astrobee 1500 becomes random in nature during two periods of flight. The first period occurred during first stage burning, from T+6 to T+25 seconds, and indicated the high acoustic environment encountered as the vehicle passed through transonic flight and the maximum dynamic pressure region. Probability density analysis (PDA) plots of this region, Figures 44 and 45, indicate a gaussian distribution. The power vs frequency distribution of the signals are shown by power spectral density (PSD) plots in Figures 46 and 47. Peak levels in g^2/Hz and peak frequencies are noted for convenience on each PSD plot plus the time interval of analysis. As can be observed from these plots, most of the random vibration energy is contained within the regions 40 Hz to 100 Hz and 700 Hz to 2000 Hz throughout the transonic region of flight. The longitudinal axis indicates a peak at 50 Hz corresponding to the longitudinal response noted at lift-off. Similarly, a peak in both lateral axes at approximately 70 Hz corresponds to the 67 Hz lateral response noted during lift-off.

A second random data region appeared directly after second stage burn-out. This also proved to have a gaussian distribution, as seen in PDA plots in Figure

48. Power spectral density plots define the frequency-power relationship for the signal during this period in Figure 49. The greater part of random vibration energy is seen to be above 120 Hz in all axes, with some below 30 Hz in the longitudinal axis. A distinct peak, at 800 Hz, is seen to occur in the yaw axis. Overall levels are relatively low.

The source of random excitation for this second region of random data has not been determined. The altitude at which this phenomenon takes place precludes an aerodynamic buffeting source for this random excitation. Since this period of random vibration occurs during second stage trail-off of burning, a possible source of this excitation is some type of irregular burning phenomenon occurring during the burn-out phase.

CONCLUDING REMARKS

All vibrations during the burning phases of the Astrobee 1500 flight were relatively low in level with the exception of a longitudinal vibration of 2.7 g at 50 Hz during first stage ignition. Maximum RMS levels for the transonic region of flight were below 1 g RMS. Most of the flight was characterized by low level transient vibrations. Some low level low frequency responses appeared in the later stages of the flight indicating coning motion.

An anomaly occurred during the flight which produced numerous structural responses in all axes. This was the opening-up and dropping-off of the clamshell heat shield without its release mechanism being activated. These responses ranged in frequency from 12.5 Hz to 1200 Hz and, in one instance, reached a maximum of 26 g's at a frequency of 1200 Hz.

Late in the flight, the second stage motor case began to unwrap, due to high motor temperatures, causing erratic motion of the vehicle. This was indicated by an 5.1 Hz response at a maximum level of 7.1 g which quickly decayed to zero.

Figure 1. Launch of Astrobee 1500 from Launcher 2 at Wallops Station, Va., October 21, 1964

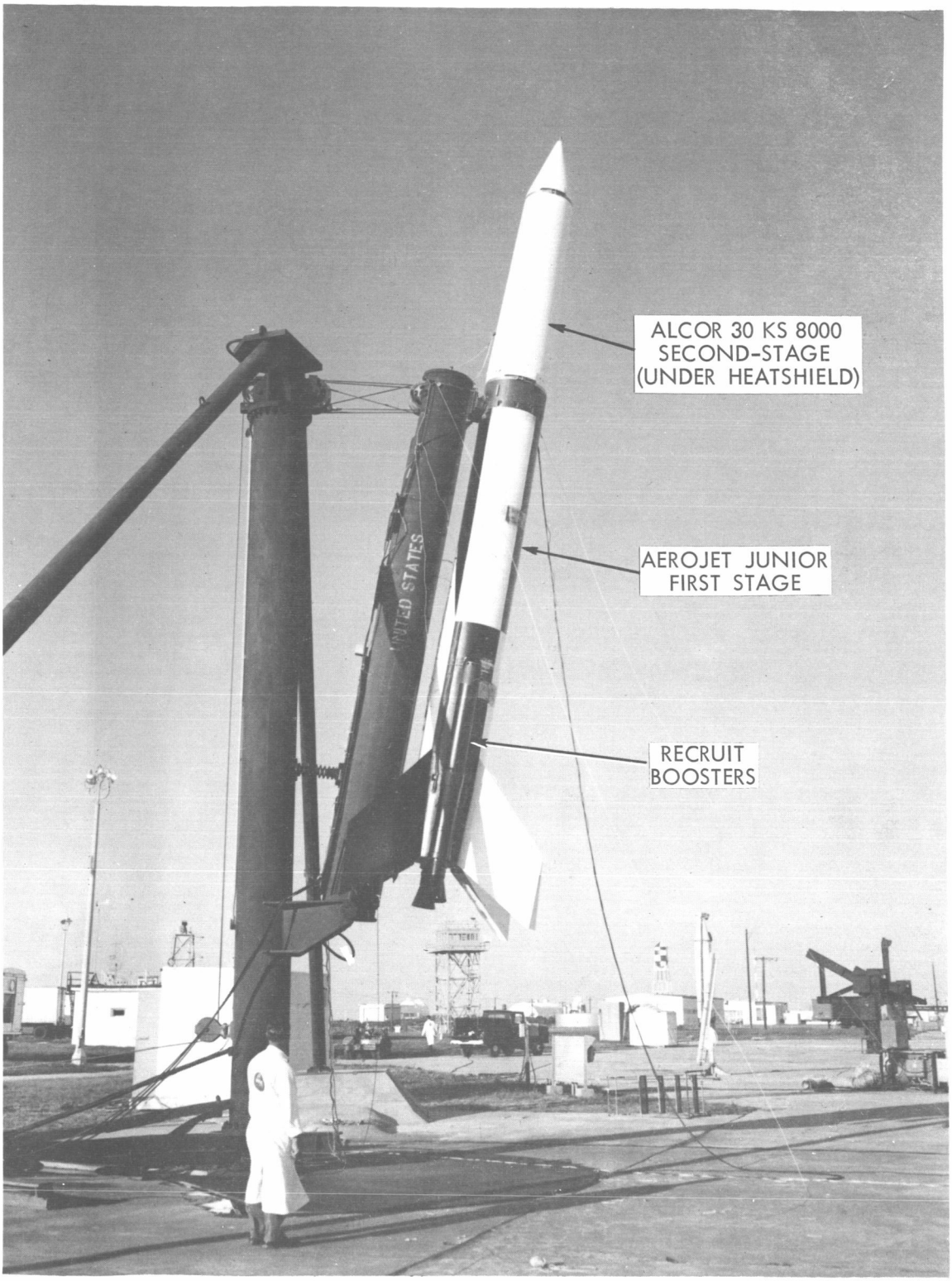

Figure 2. Astrobee 1500, NASA 16.02 on Tubular Launcher, October 21, 1964

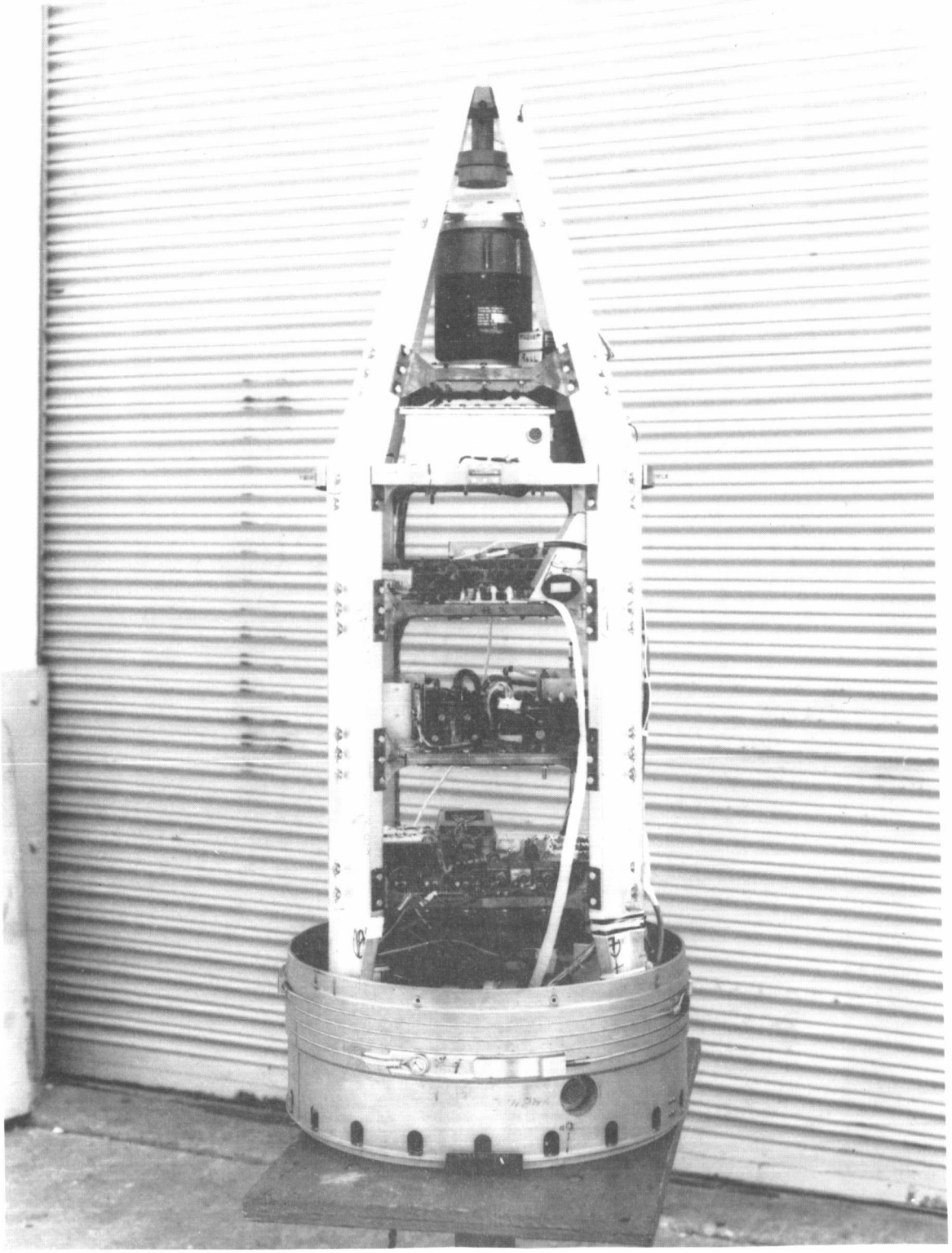

Figure 3. Astrobee 1500 Payload Before Installation on Rocket

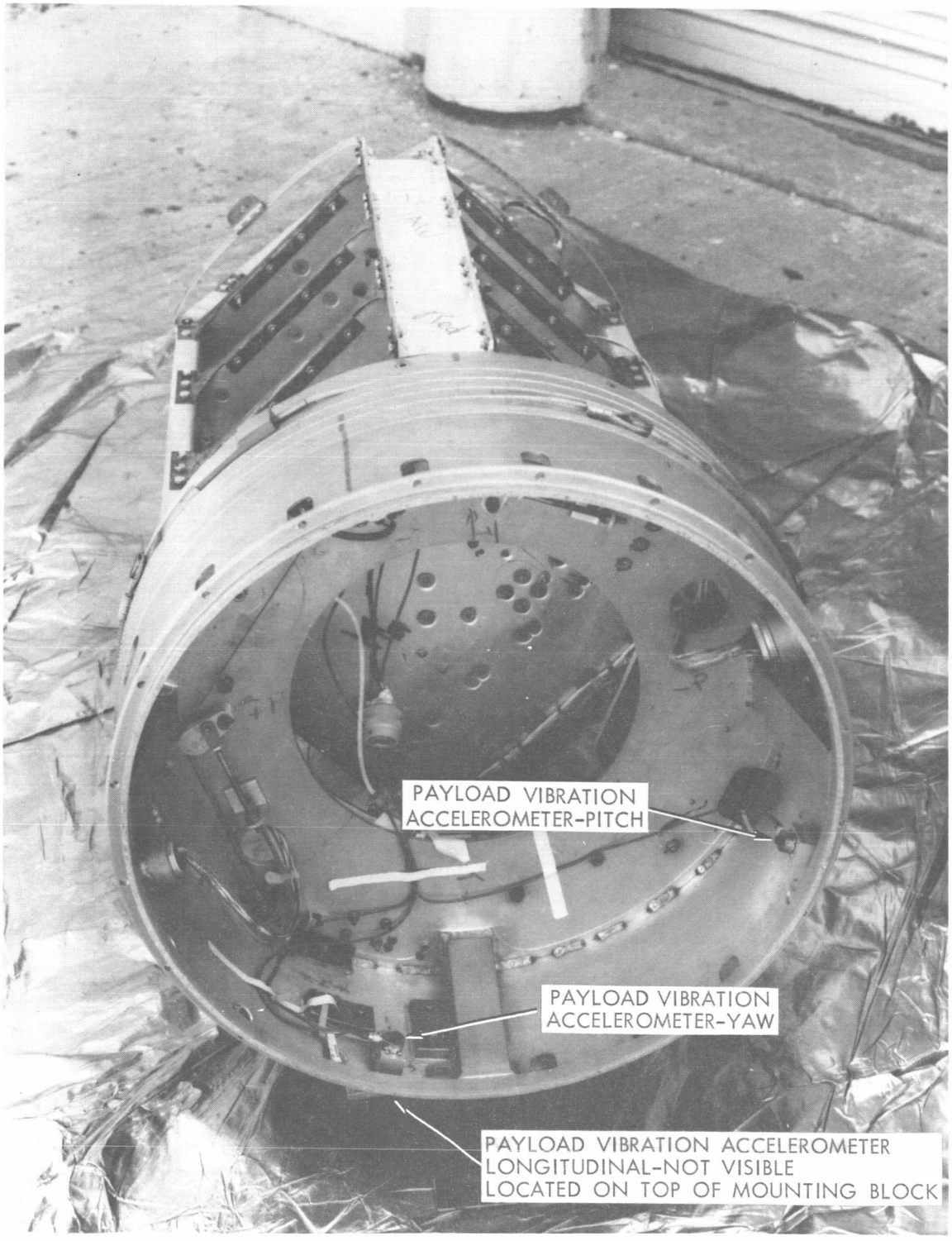

Figure 4. Position of Vibration Experiment on Astrobee 1500 Payload

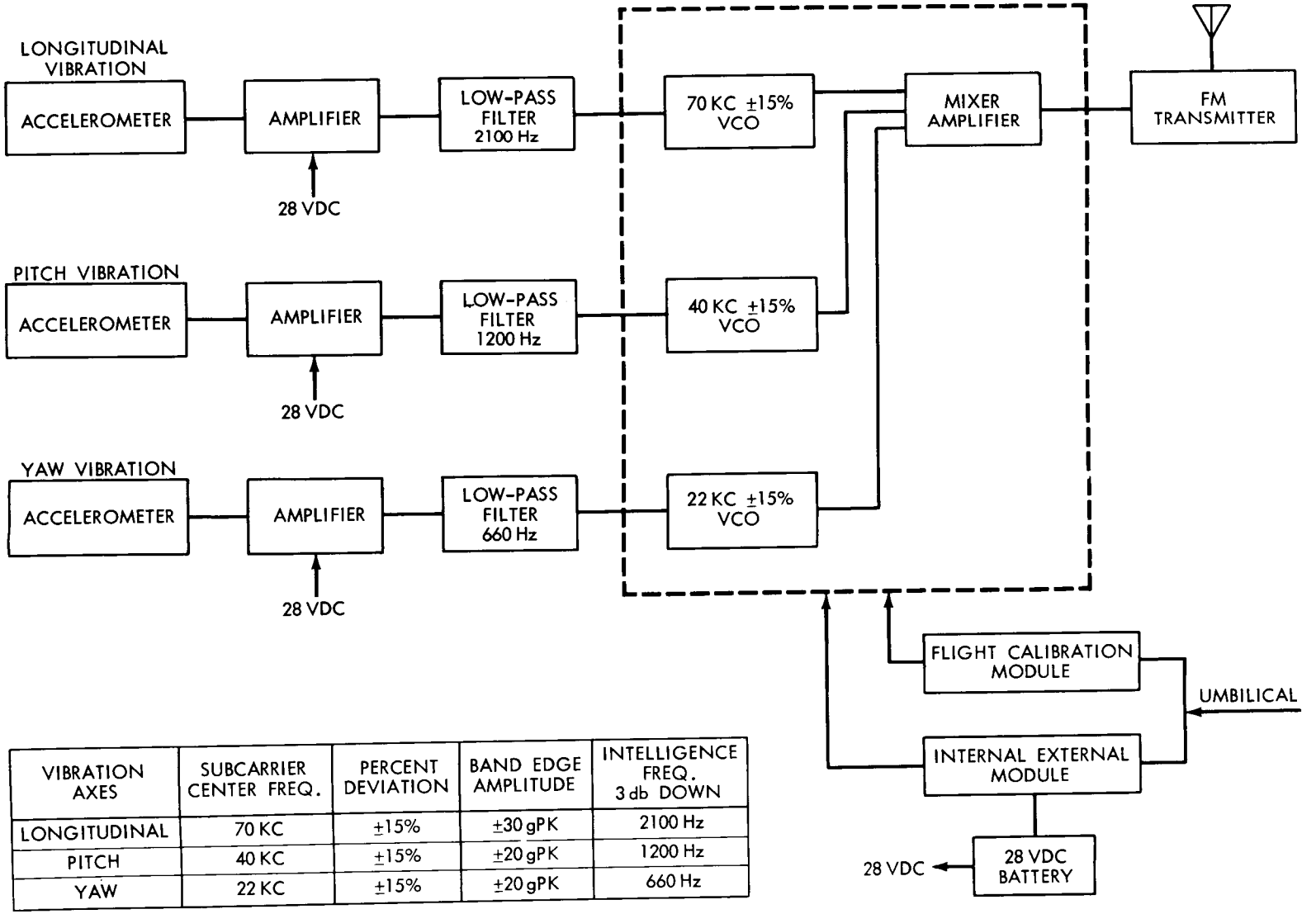

VIBRATION AXES	SUBCARRIER CENTER FREQ.	PERCENT DEVIATION	BAND EDGE AMPLITUDE	INTELLIGENCE FREQ. 3 db DOWN
LONGITUDINAL	70 KC	±15%	±30 gPK	2100 Hz
PITCH	40 KC	±15%	±20 gPK	1200 Hz
YAW	22 KC	±15%	±20 gPK	660 Hz

Figure 5. Vibration Measuring System

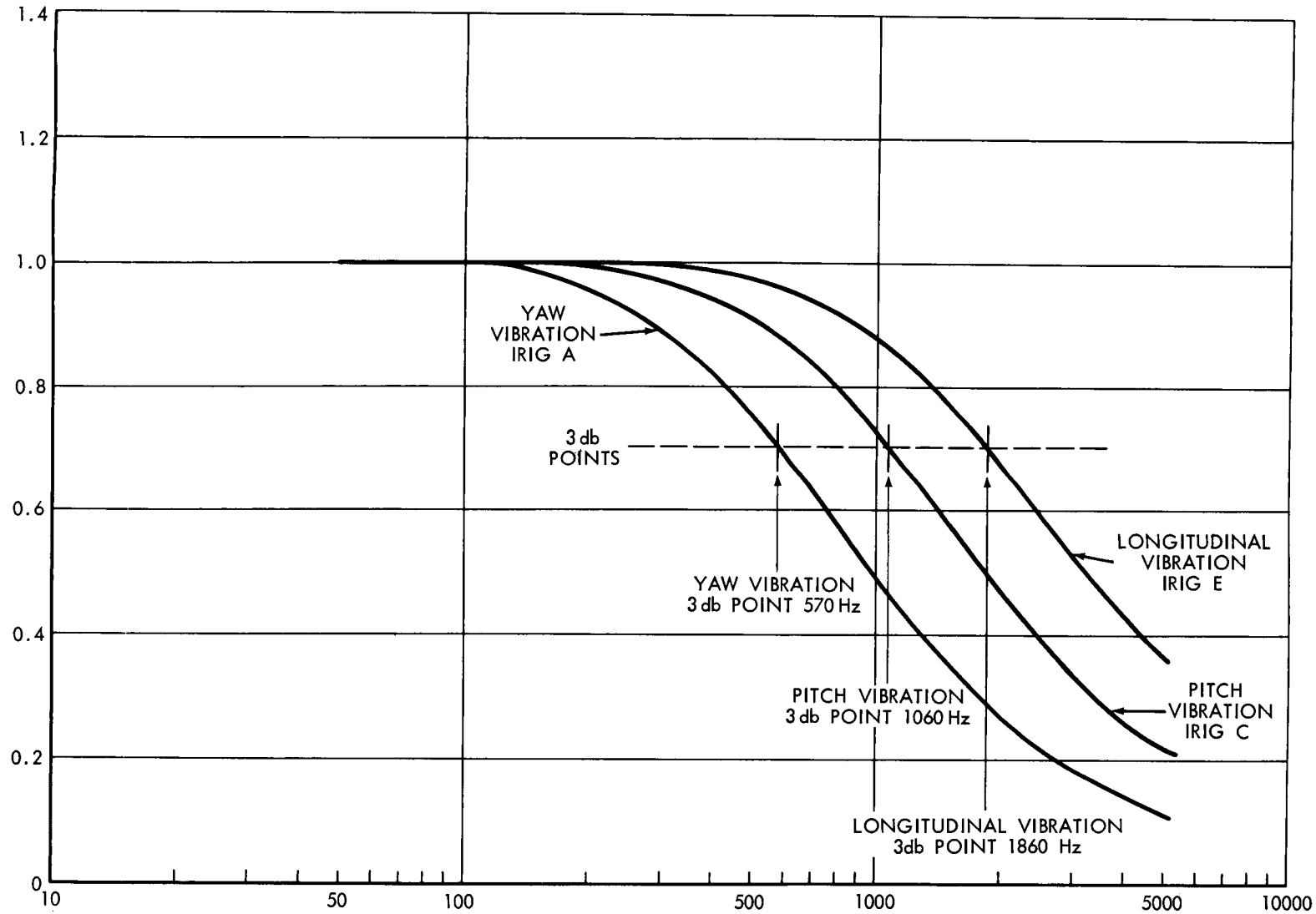

Figure 6. System Frequency Response

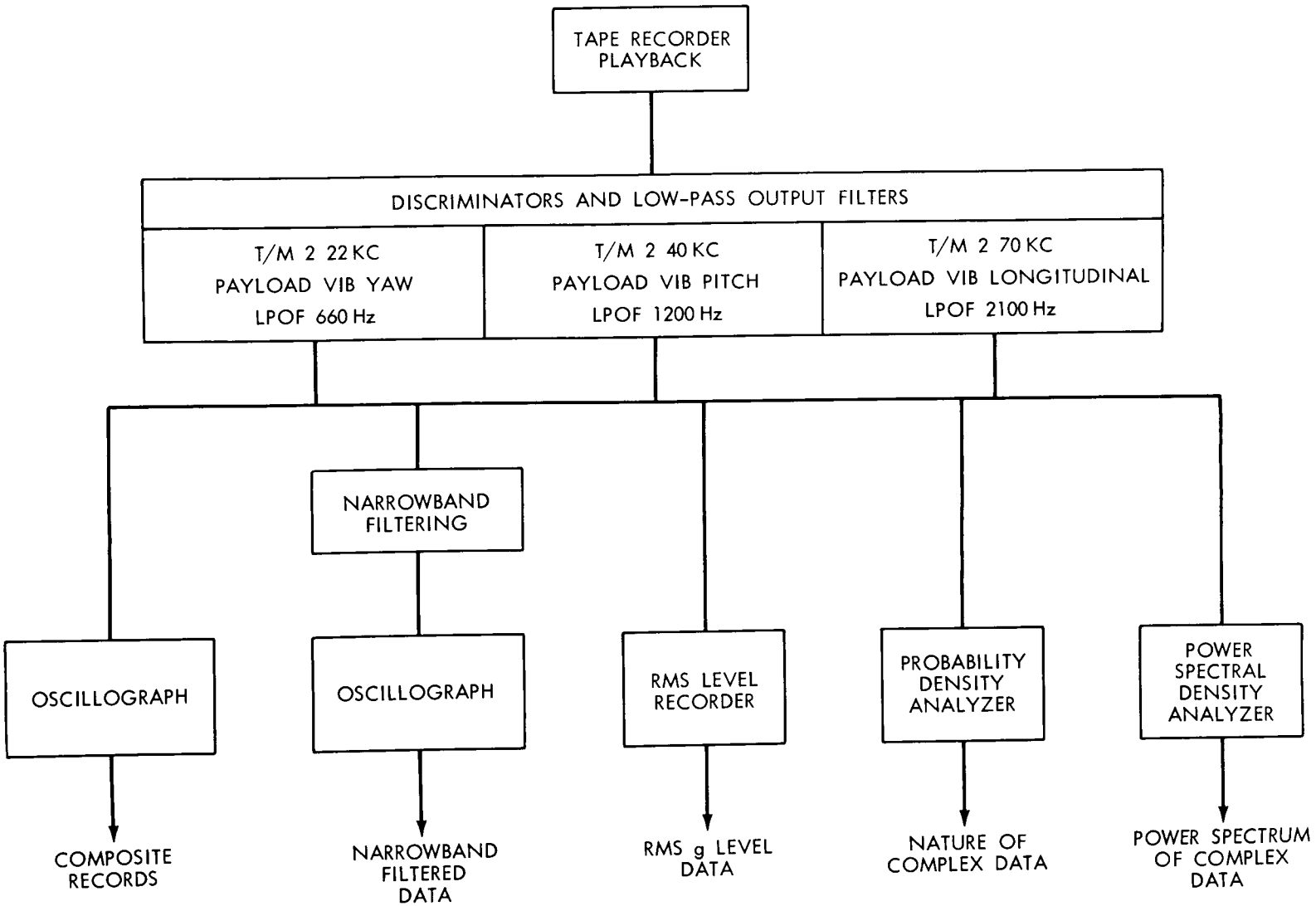

Figure 7. Vibration Data-Reduction System

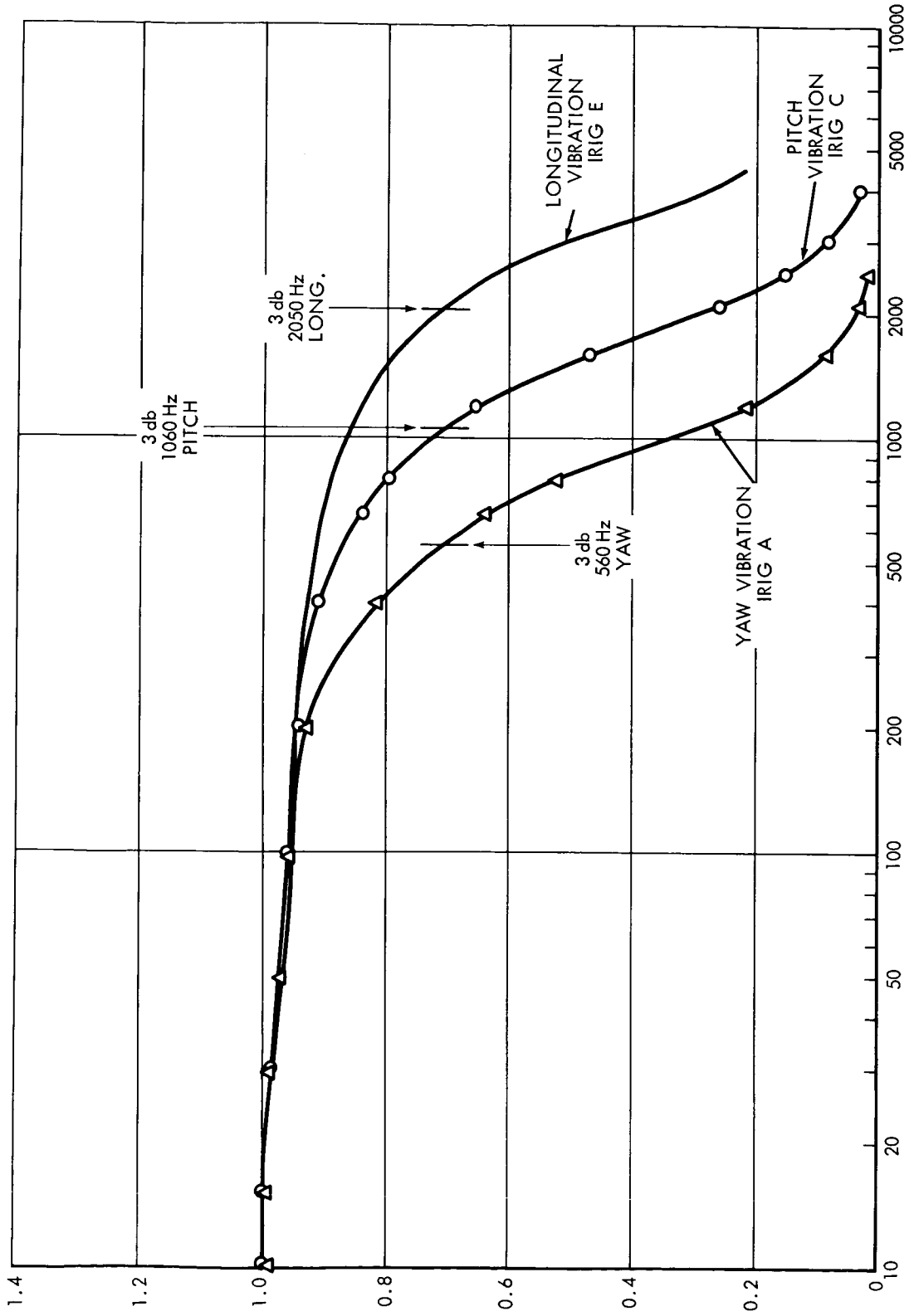

Figure 8. Frequency Response of Total Playback System

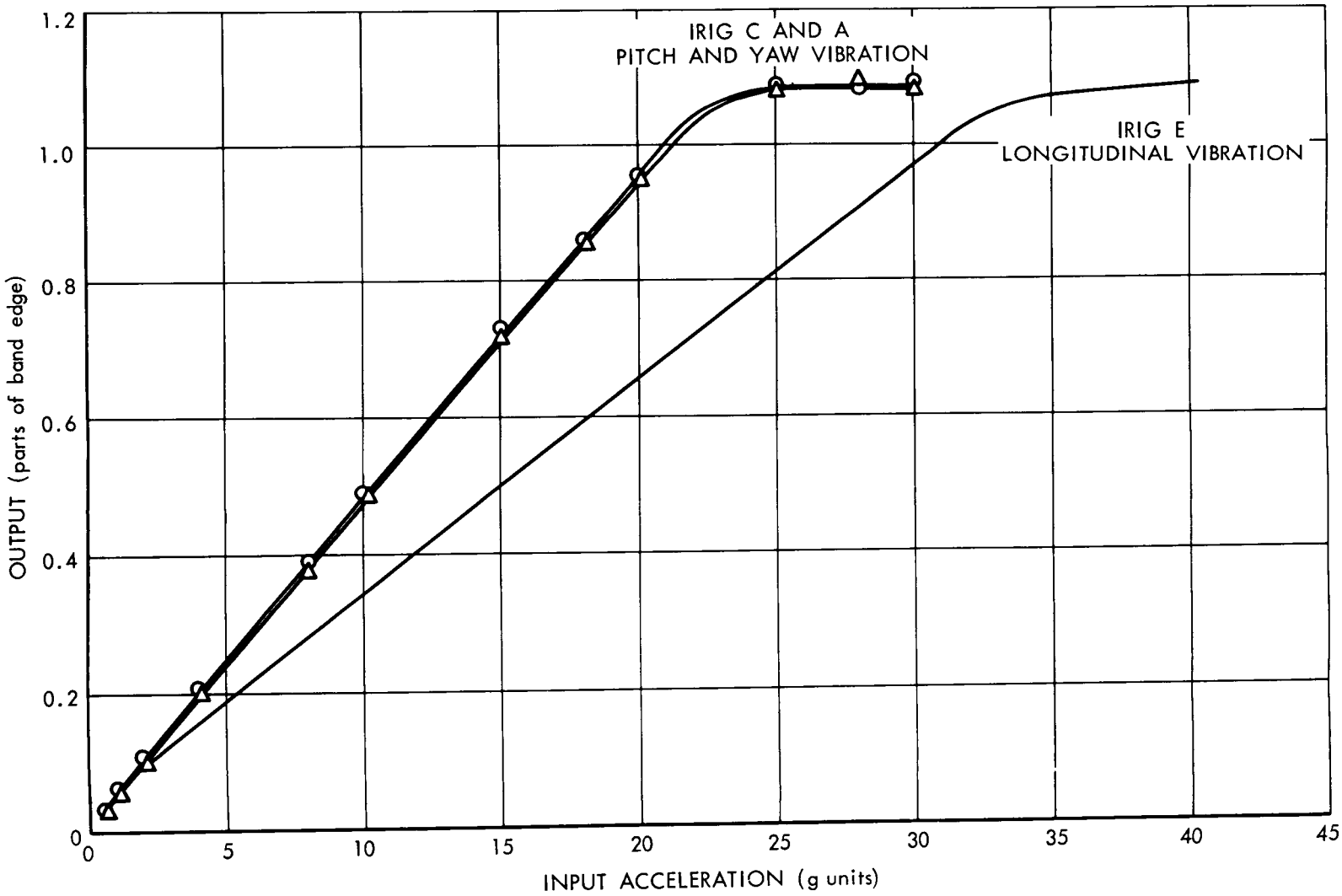

Figure 9. Amplitude Linearity Response of Total Playback System

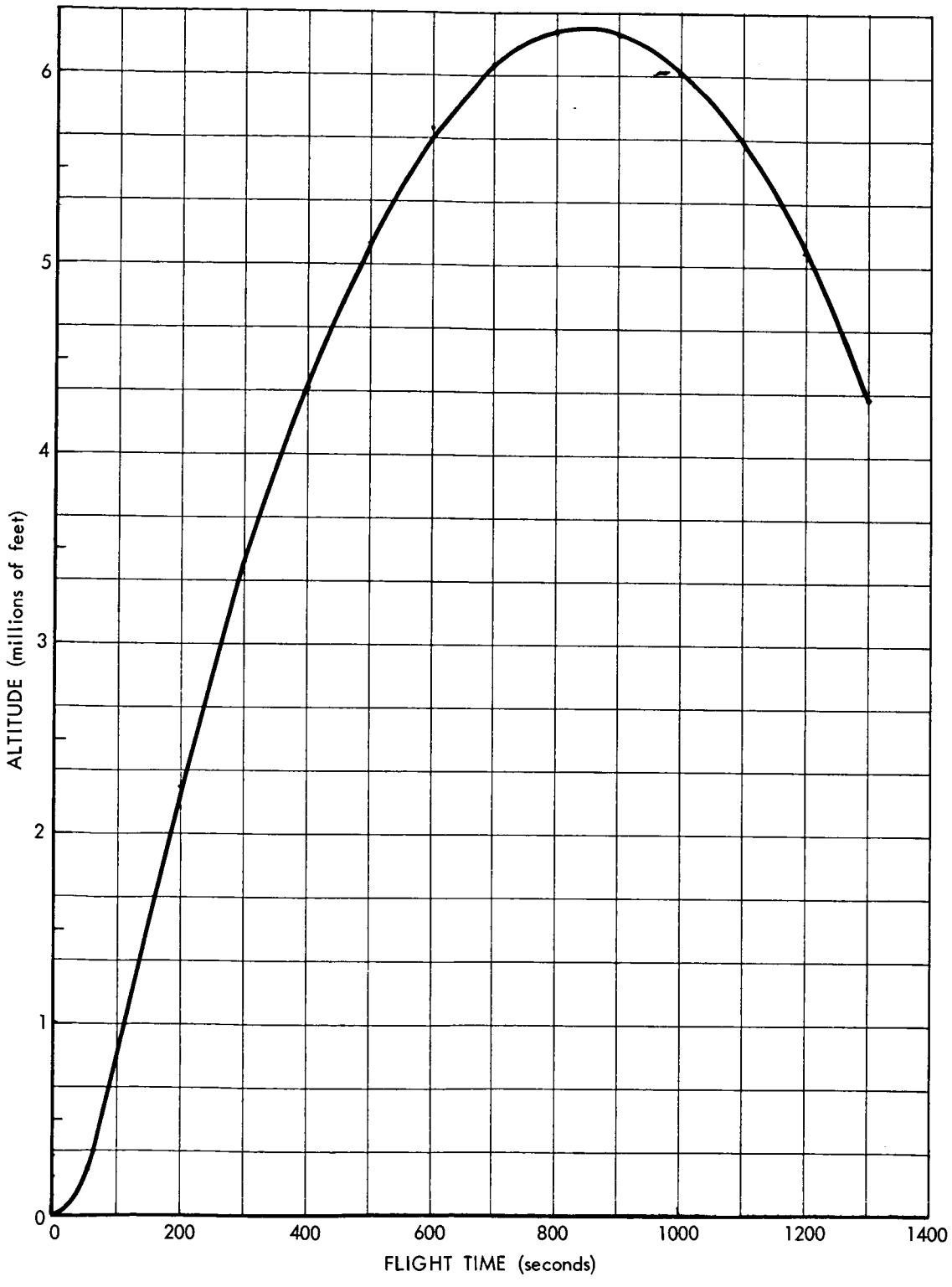

Figure 10. Altitude vs Flight Time

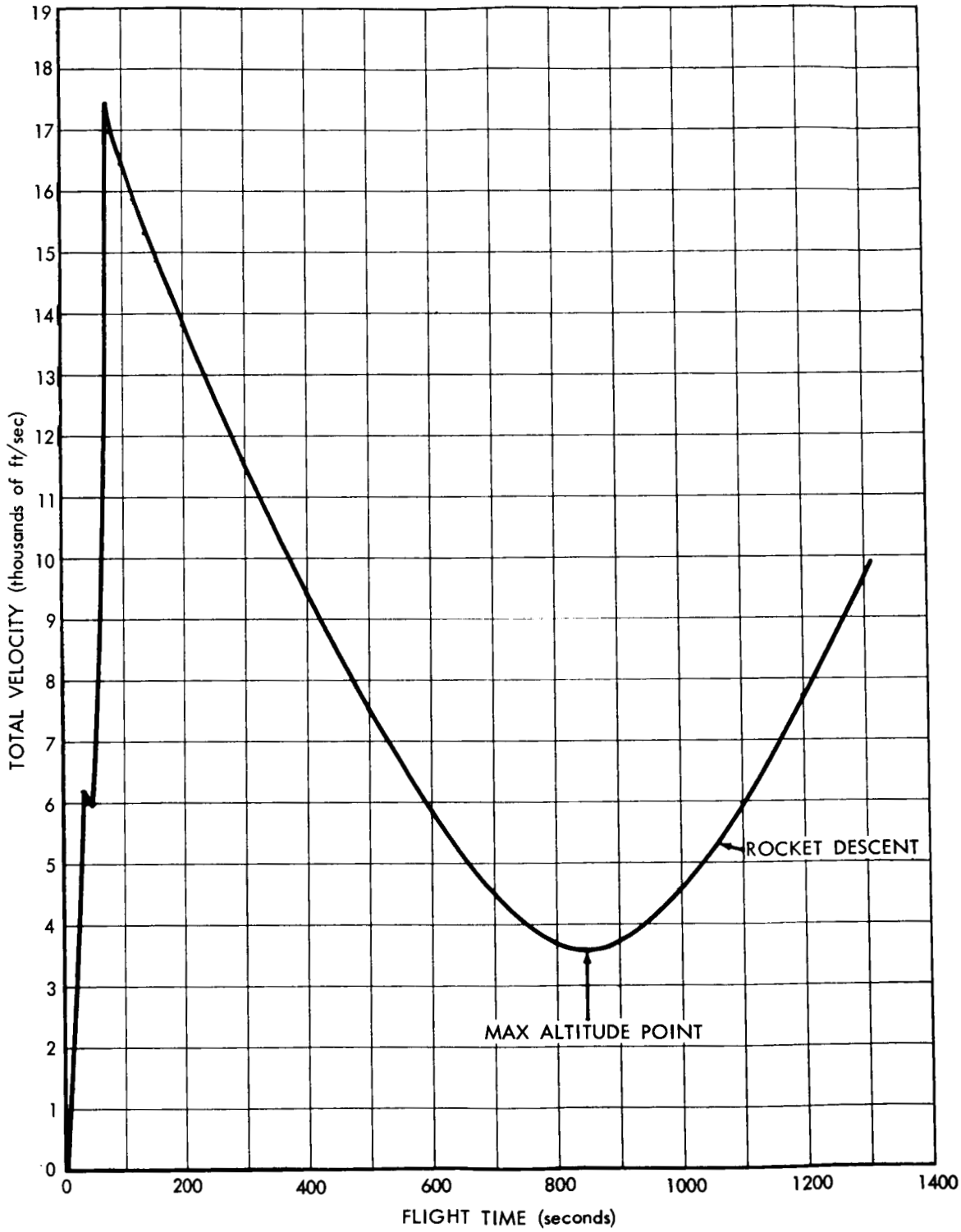

Figure 11. Total Vehicle Velocity vs Flight Time

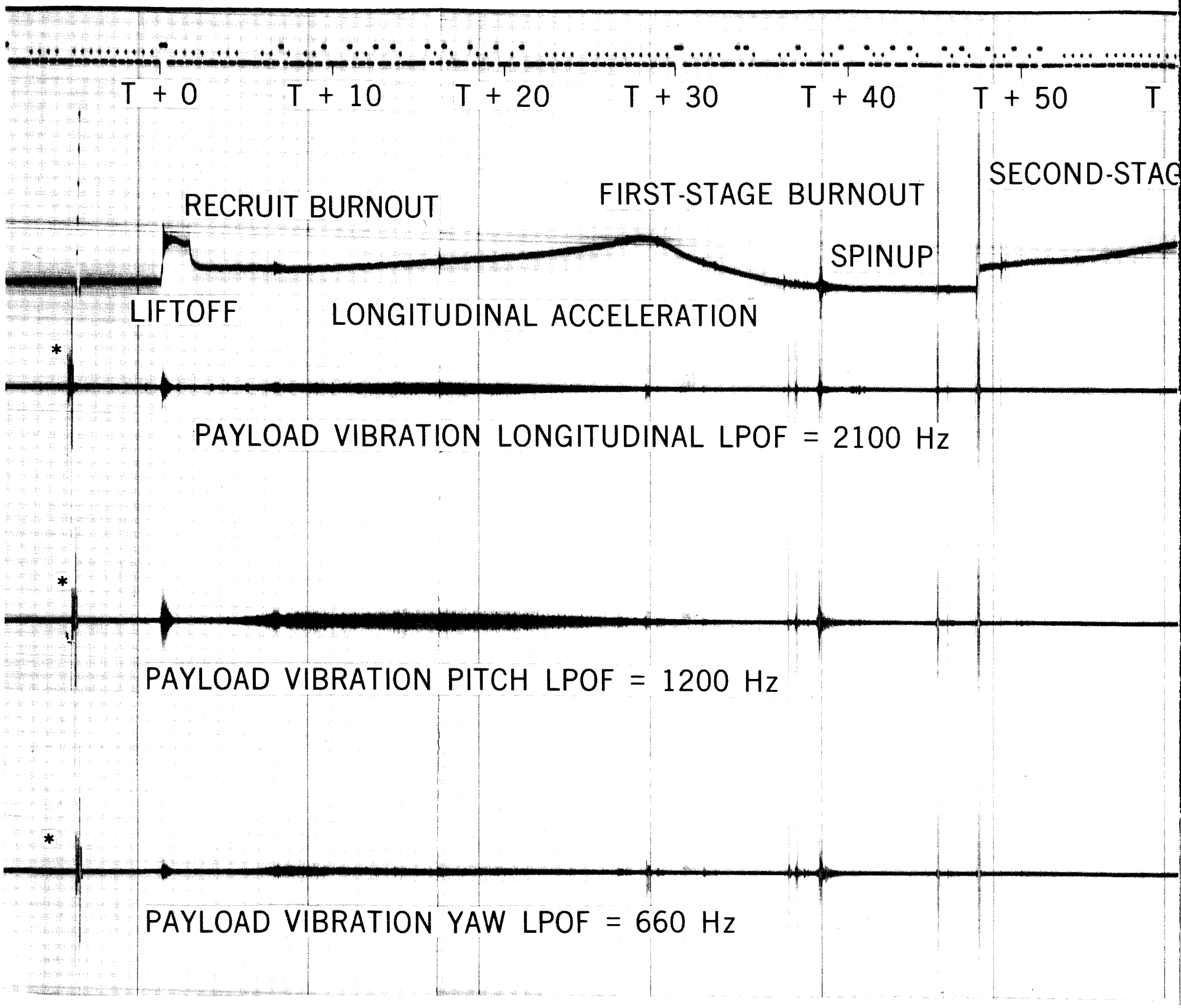

FOLDOUT FRAME 1

FOLDOUT FRAME 2

1

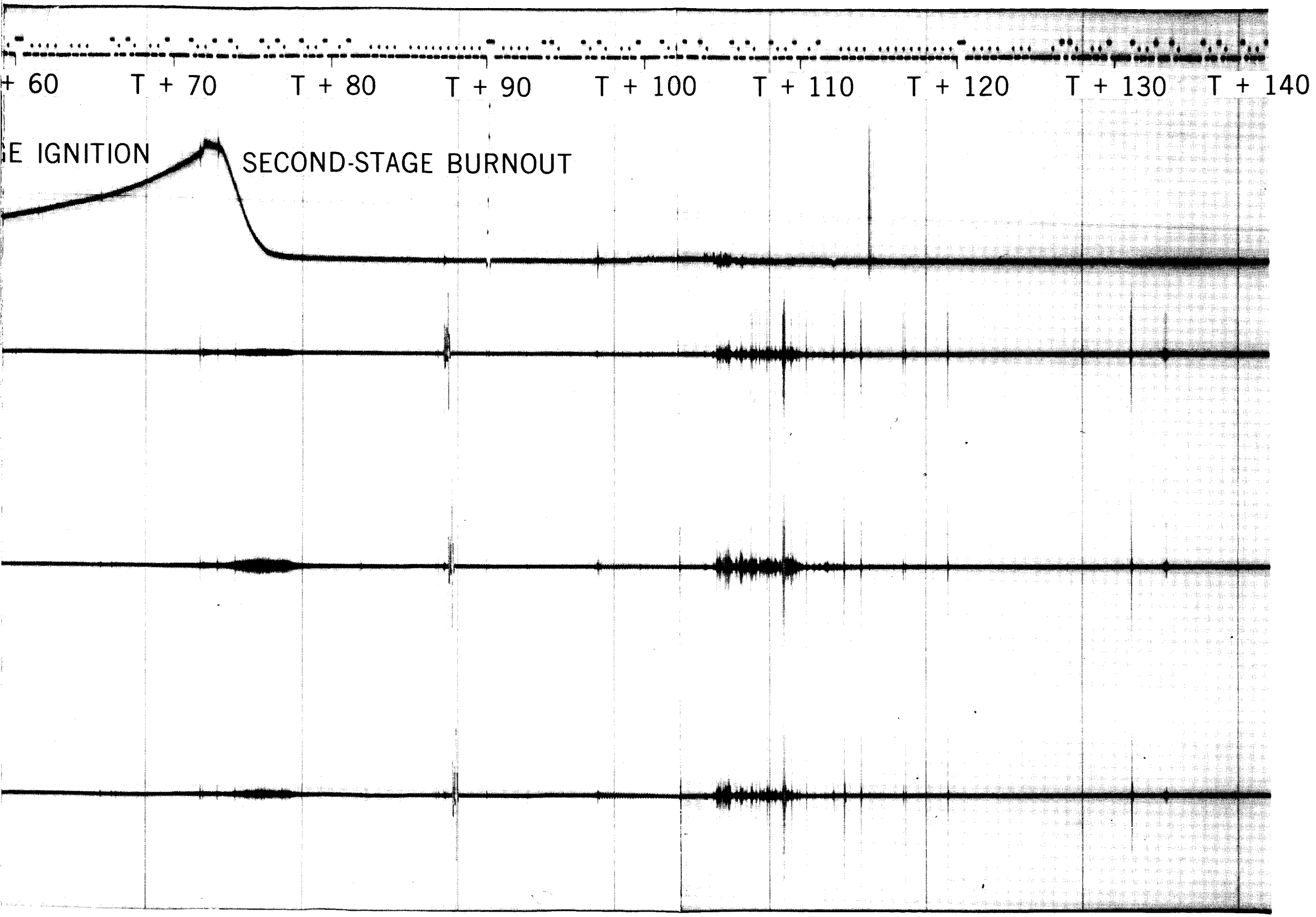

Figure 12. Overall Vibration Time History

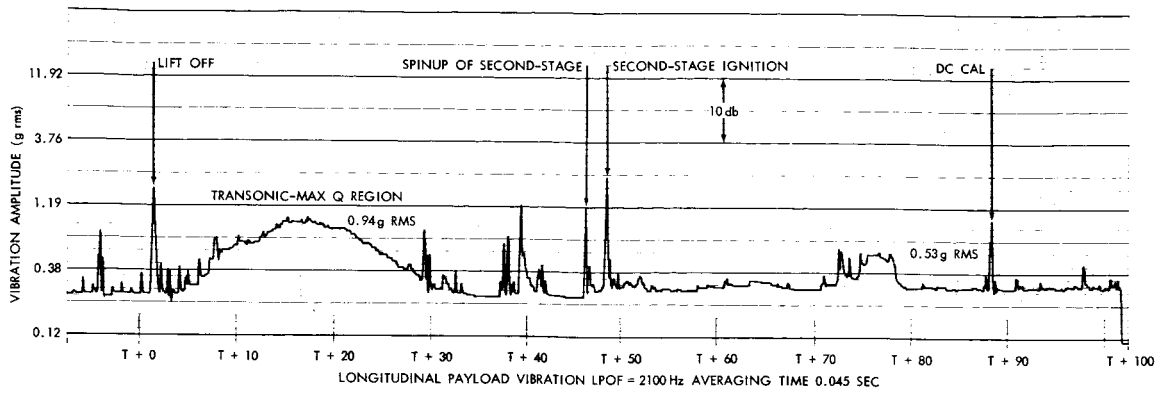

Figure 13. Payload Longitudinal Vibration rms Level Time History

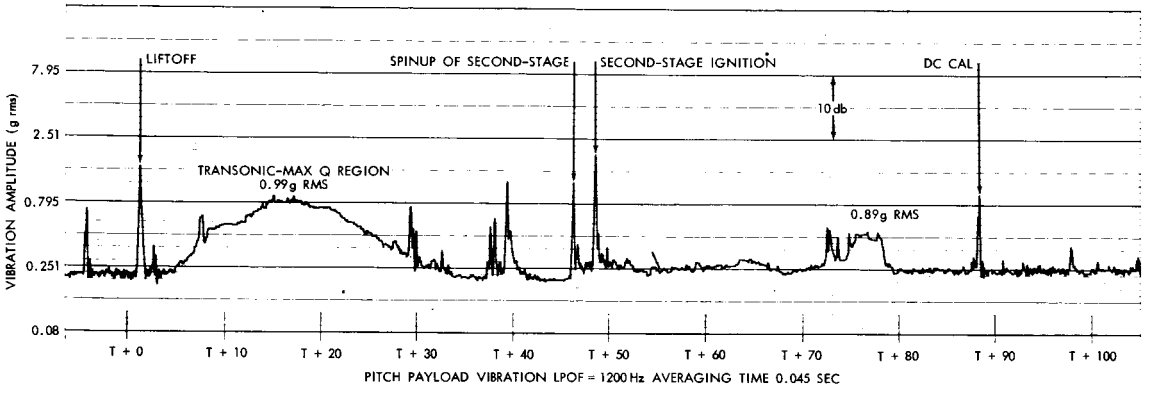

Figure 14. Payload Pitch Vibration rms Level Time History

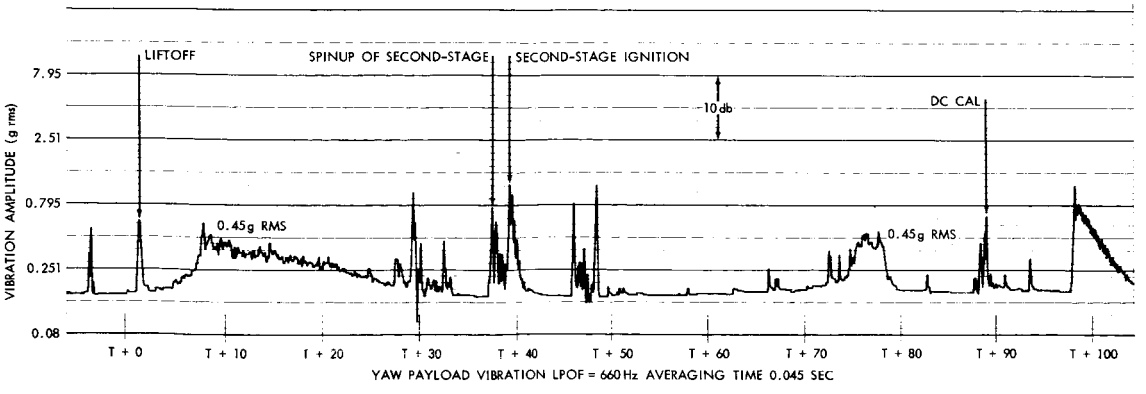

Figure 15. Payload Yaw Vibration rms Level Time History

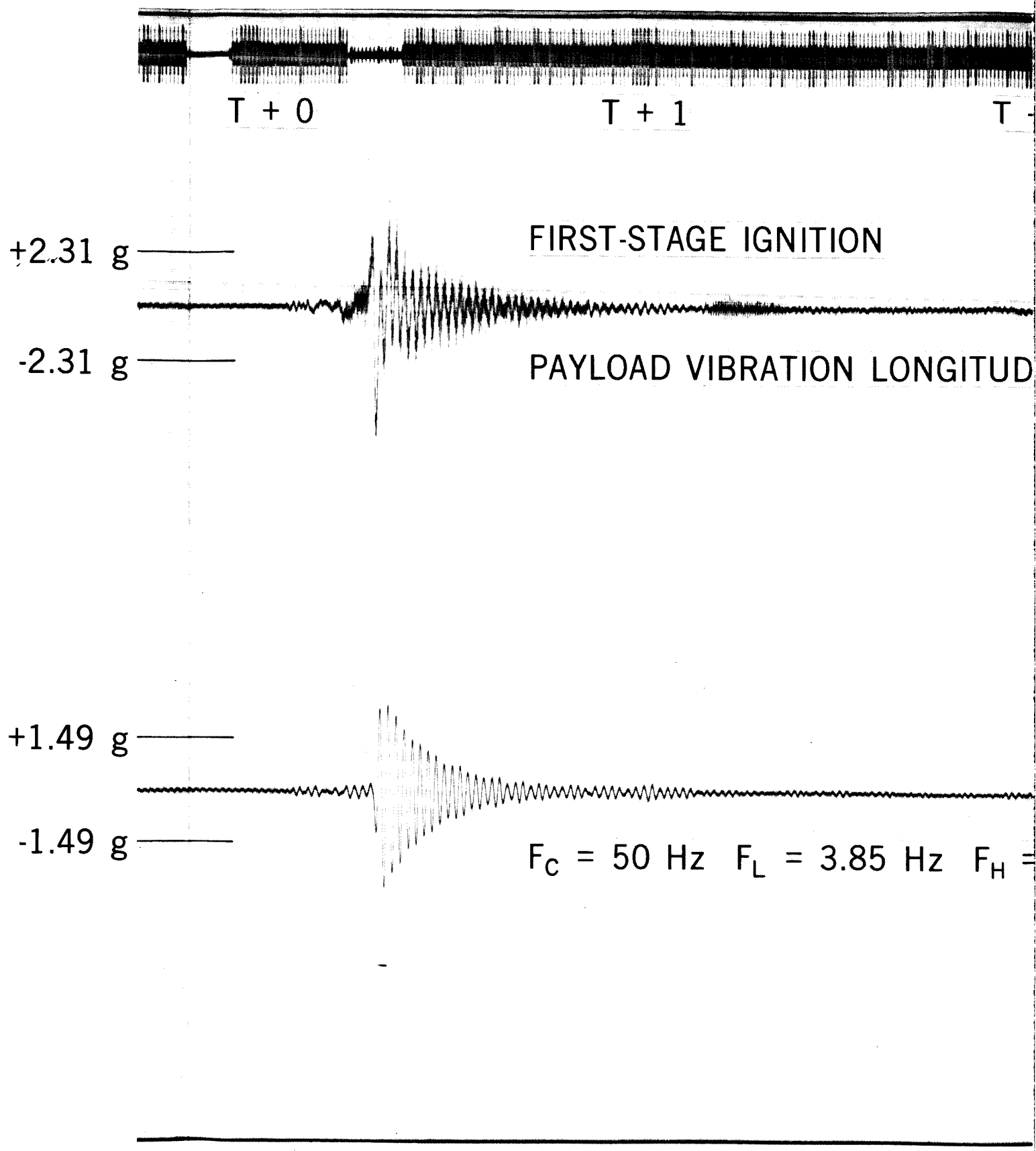

Figure 16. Longitudinal Vibration, Liftoff, T + 0 : 50 Hz

FOLDOUT FRAME 1 PRECEDING PAGE BLANK NOT FILMED. FOLDOUT FRAME 1

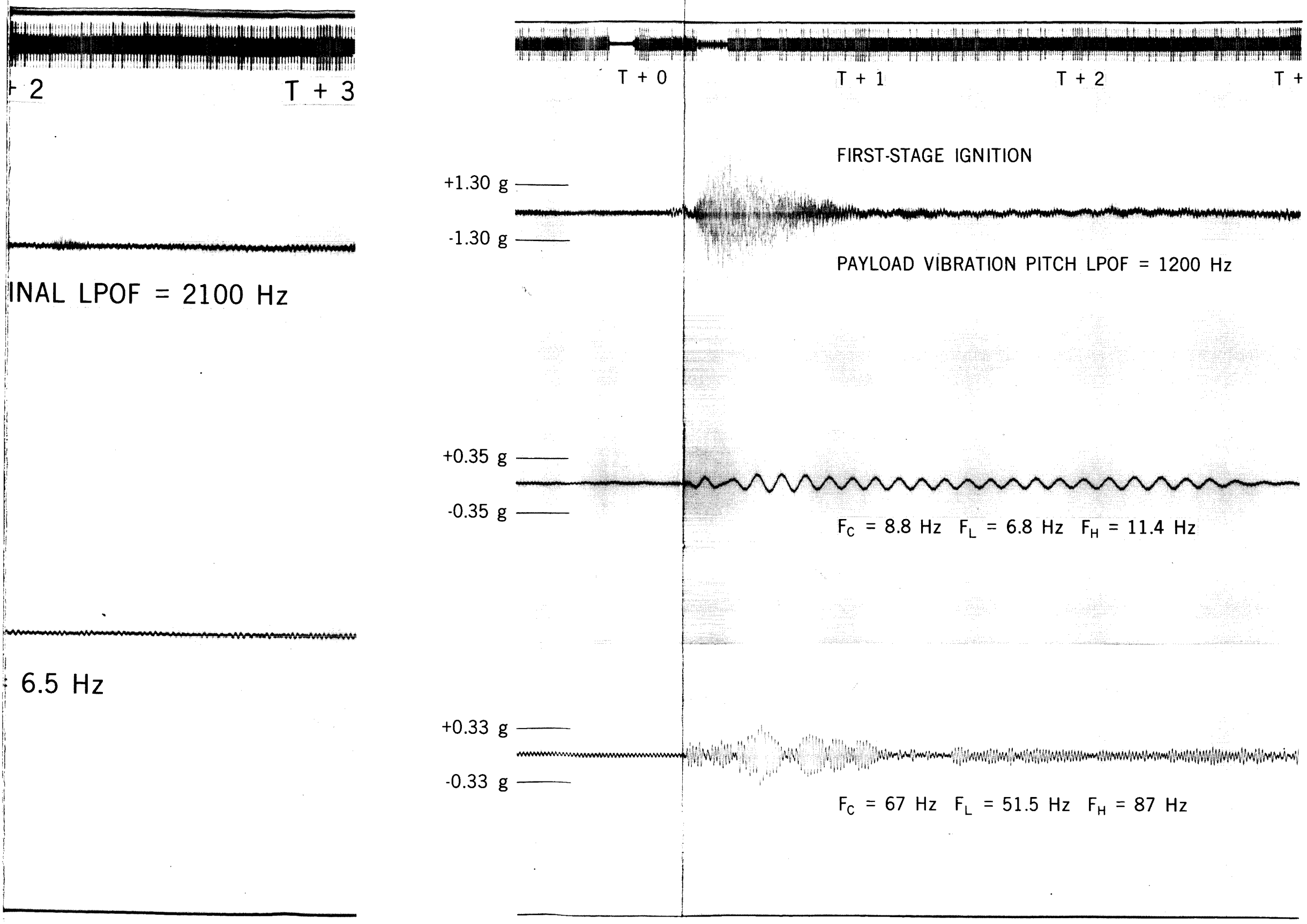

Figure 17. Pitch Vibration, Liftoff, T + 0 : 67 and 9.3 Hz

FOLDOUT FRAME 2

FOLDOUT FRAME 3

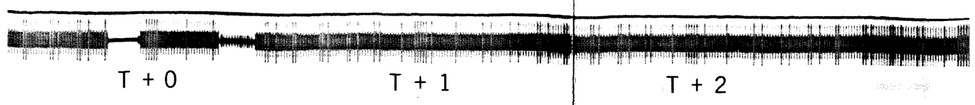

PAYLOAD VIBRATION YAW LPOF = 660 Hz

F_C = 67 Hz F_L = 51.5 Hz F_H = 87 Hz

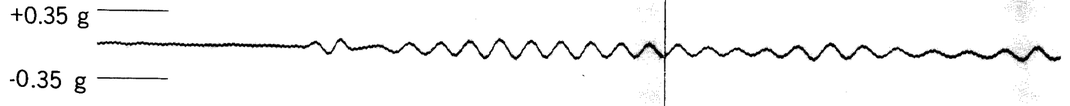

F_C = 8.5 Hz F_L = 6.5 Hz F_H = 11 Hz

Figure 18. Yaw Vibration, Liftoff, T + 0 : 67 and 9.3 Hz

FOLDOUT FRAME 1

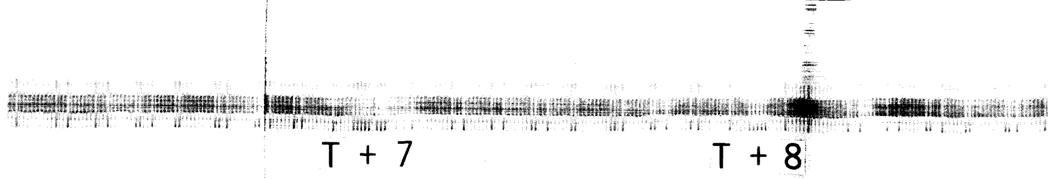

FIRST-STAGE BURN IRREGULARITY AT T + 6.7 SECONDS

PAYLOAD VIBRATION LONGITUDINAL LPOF = 2100 Hz

F_C = 50 Hz F_L = 38 Hz F_H = 65 Hz

Figure 19. Longitudinal Vibration, Transonic Flight, T + 6.7 Sec : 50 Hz

FOLDOUT FRAME 2

FOLDOUT FRAME 3

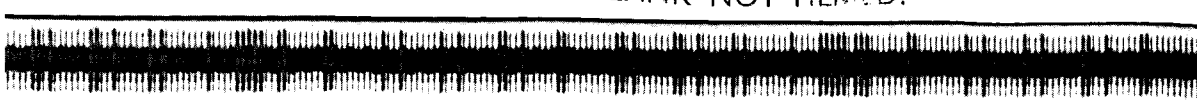

T + 16 T + 17

FIRST-STAGE BURN IRREGULARITY AT T + 16.3 S

+1.92 g

-1.92 g

PAYLOAD VIBRATION LONGITUDINAL LPOF = 21

+0.51 g

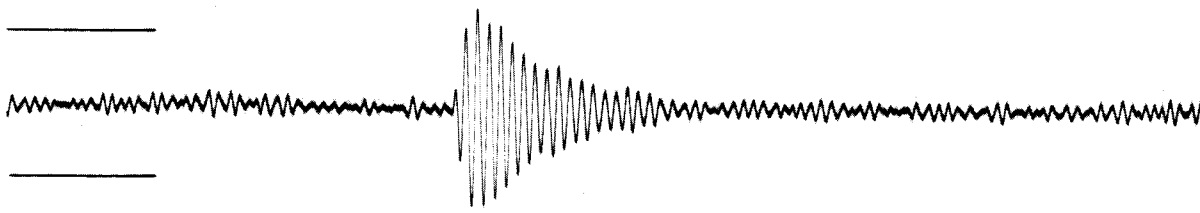

-0.51 g

F_C = 50 Hz F_L = 38 Hz F_H = 65 Hz

Figure 20. Longitudinal Vibration, Transonic Flight, T + 16.3 Sec : 50 Hz

FOLDOUT FRAME 1

FOLDOUT FRAME

T +

T + 31

T + 32

T + 33

ECONDS

+1.30 g

-1.30 g

00 Hz

PAYLOAD VIBRATION PITCH LPOF = 1200 Hz

+0.36 g

-0.36 g

F_C = 11.5 Hz F_L = 8.85 Hz F_H = 15 Hz

Figure 21. Pitch Vibration, First-Stage Burn, T + 31.6 Sec : 12 Hz

FOLDOUT FRAME 2

FOLDOUT FRAME 3

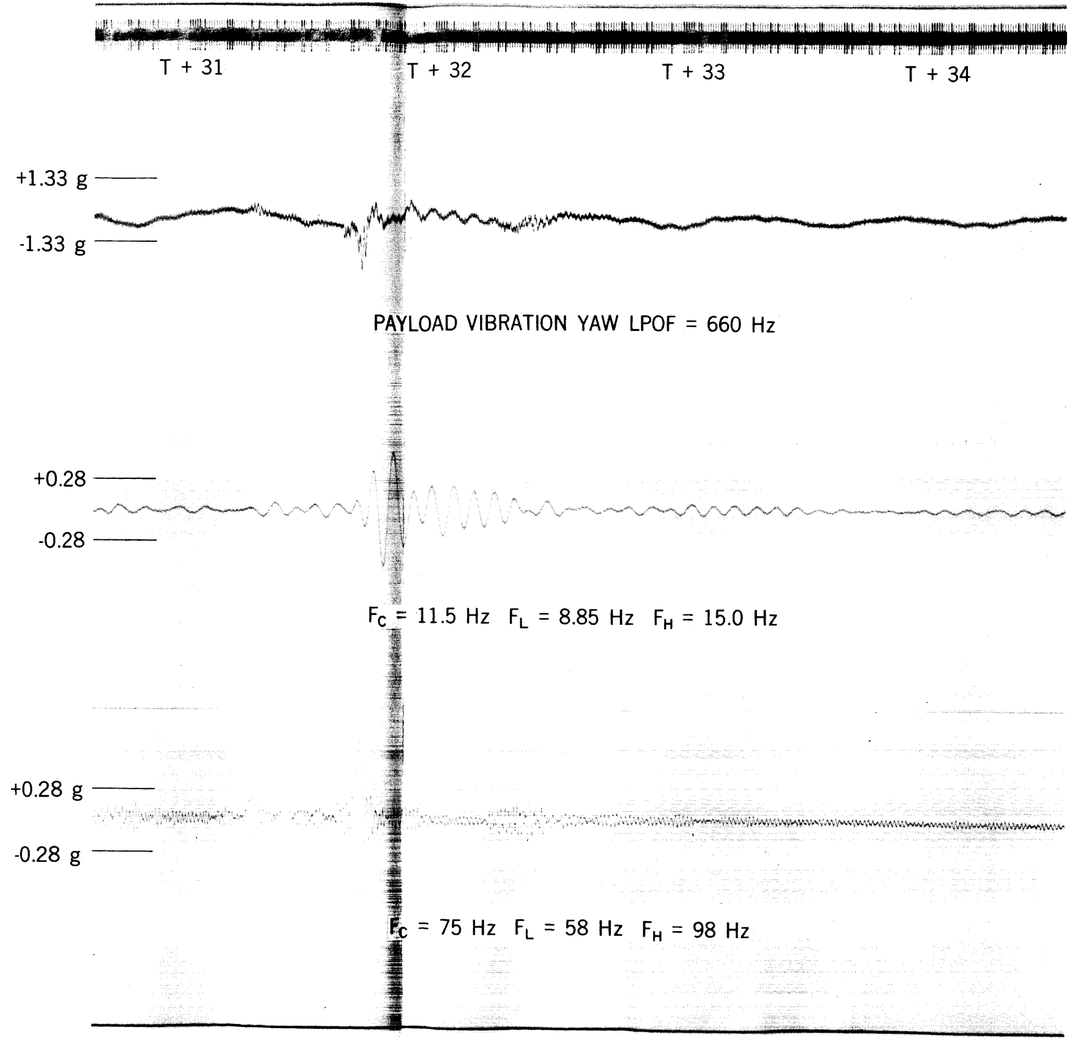

Figure 22. Yaw Vibration, First-Stage Burn, T + 31.6 Sec : 75 and 12 Hz

FOLDOUT FRAME I

PRECEDING PAGE BLANK NOT FILMED.

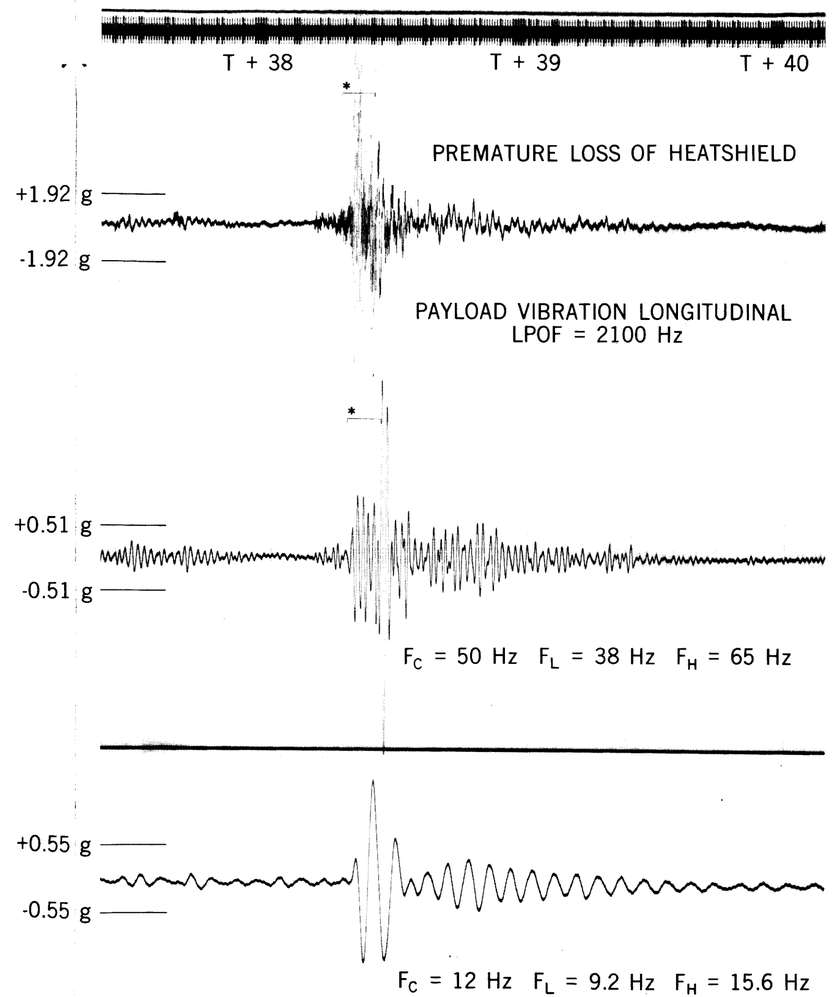

Figure 23. Longitudinal Vibration, Premature Heatshield Release, T + 38.4 Sec : 56 and 11.5 Hz

FOLDOUT FRAME II

T + 38.2 T + 38.3 T + 38.4

*

+2.72 g ———

-2.72 g ———

PAYLOAD VIBRATION LONGITUDINAL LPOF = 2100 Hz

*

+1.56 g ———

-1.56 g ———

F_C = 790 Hz F_L = 610 Hz F_H = 1050 Hz

Figure 24. Longitudinal Vibration, Premature Heatshield Release, T + 38.4 Sec : 790 Hz

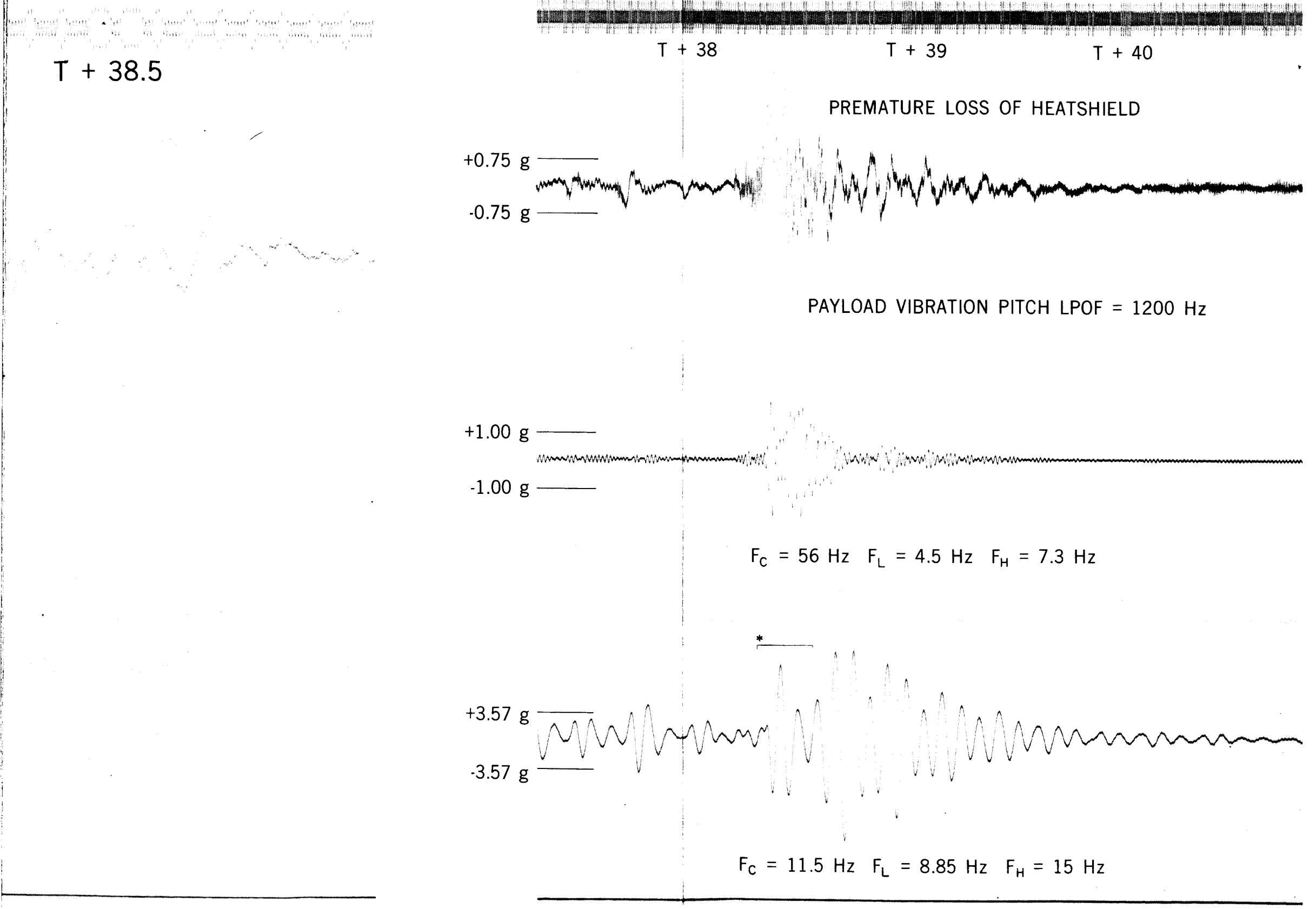

Figure 25. Pitch Vibration, Premature Heatshield Release, T + 38.4 Sec : 56 and 11.5 Hz

FOLDOUT FRAME

FOLDOUT FRAME

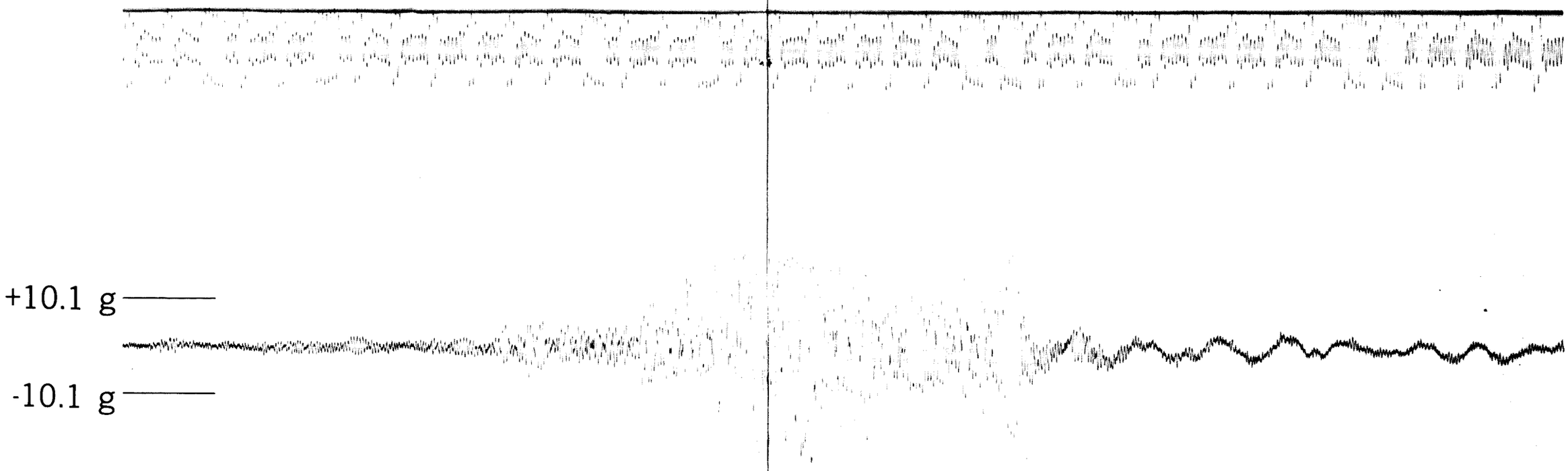

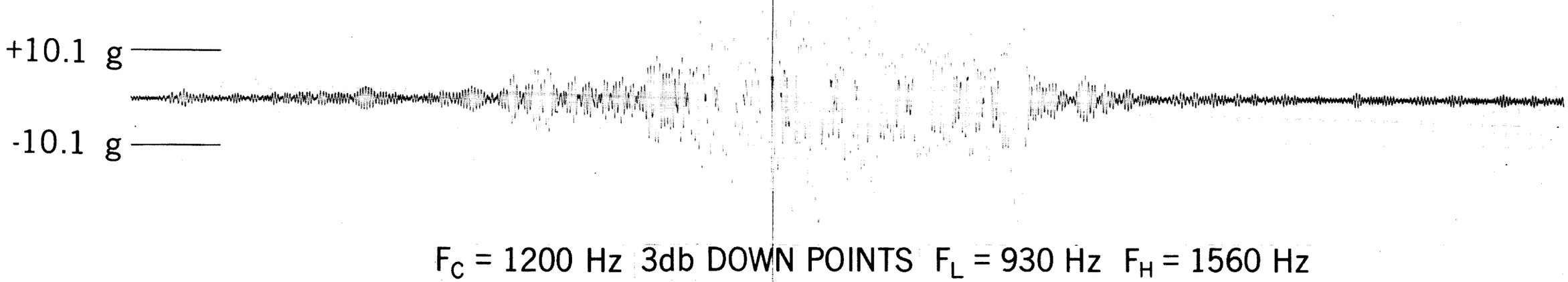

Figure 26. Pitch Vibration, Premature Heatshield Release, T + 38.4 Sec : 1200 Hz

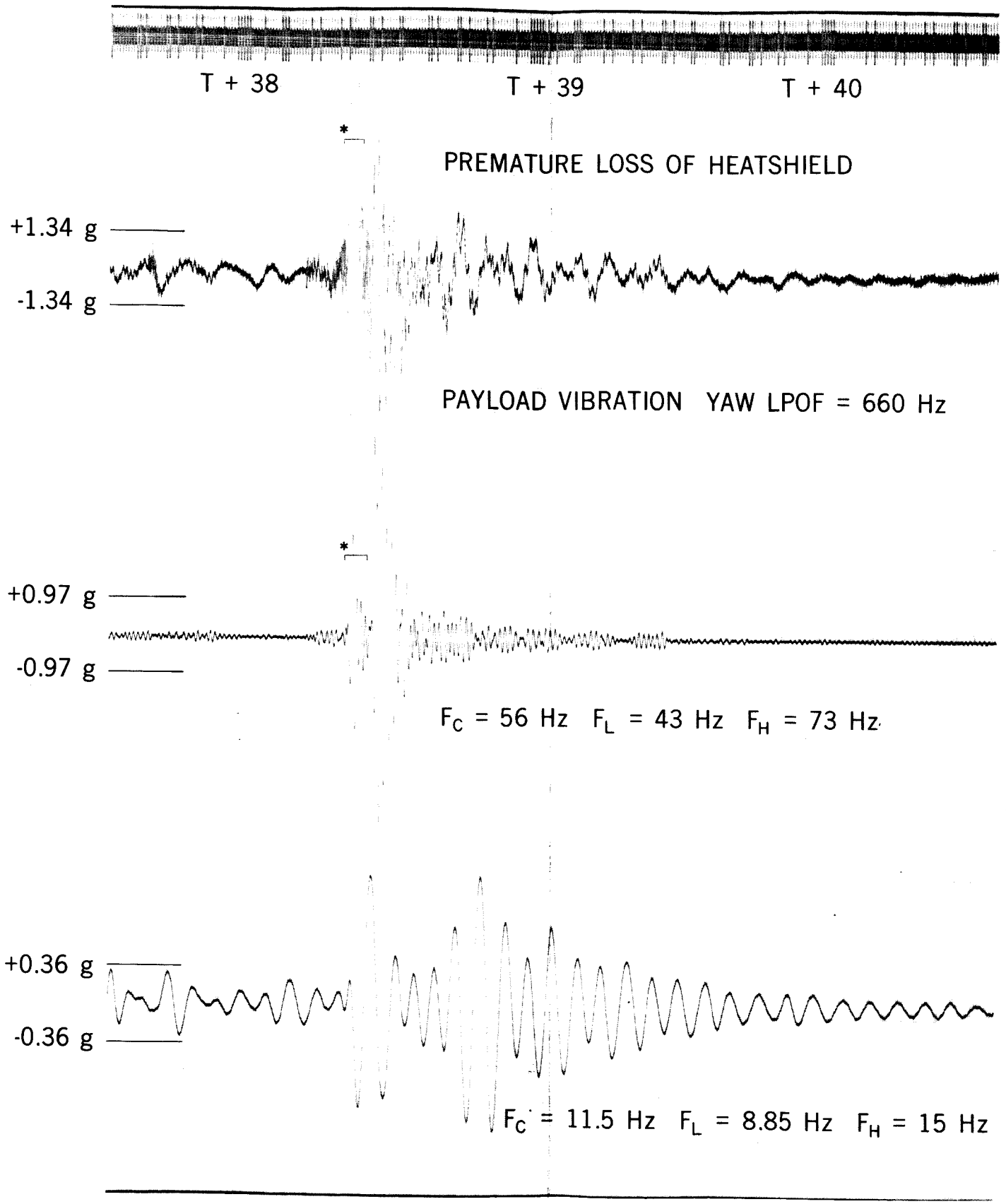

Figure 27. Yaw Vibration, Premature Heatshield Release, T + 38.4 Sec : 56 and 11.5 Hz

T + 38.2 T + 38.3 T + 38.4 T + 38.5

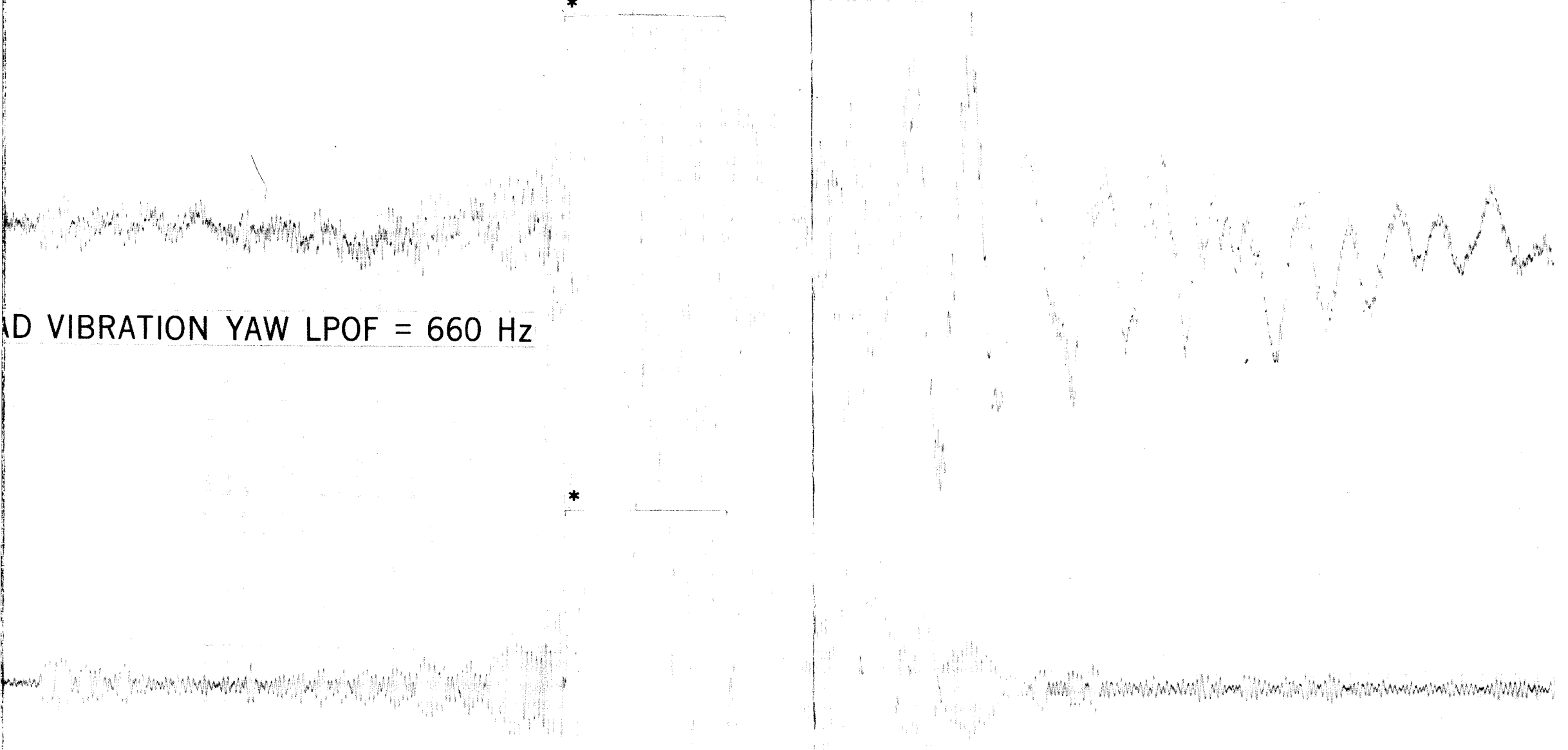

Figure 28. Yaw Vibration, Premature Heatshield Release, T + 38.4 Sec : 790 Hz

FOLDOUT FRAME

FOLDOUT FRAME

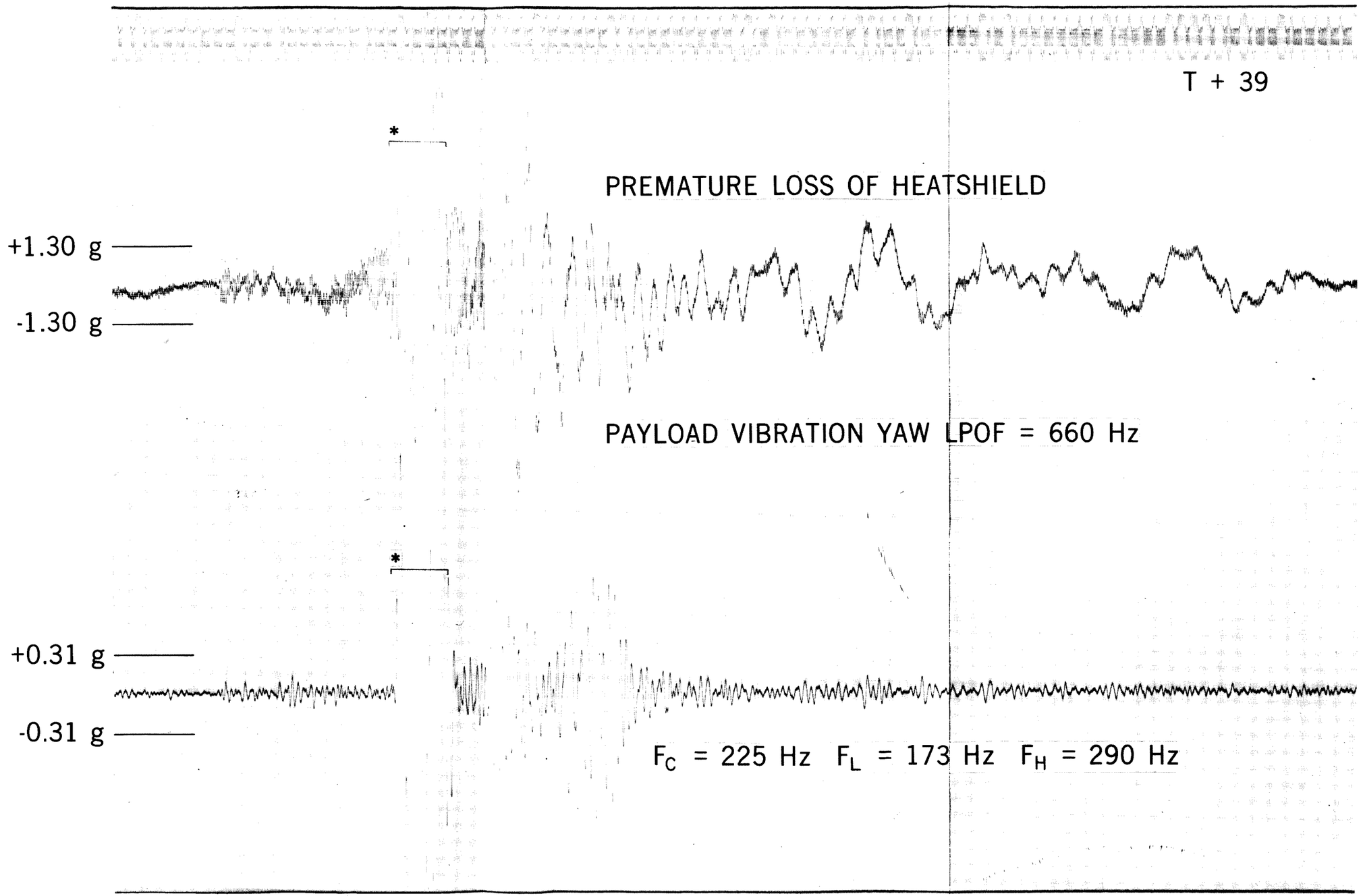

Figure 29. Yaw Vibration, Premature Heatshield Release, T + 38.5 Sec : 225 Hz

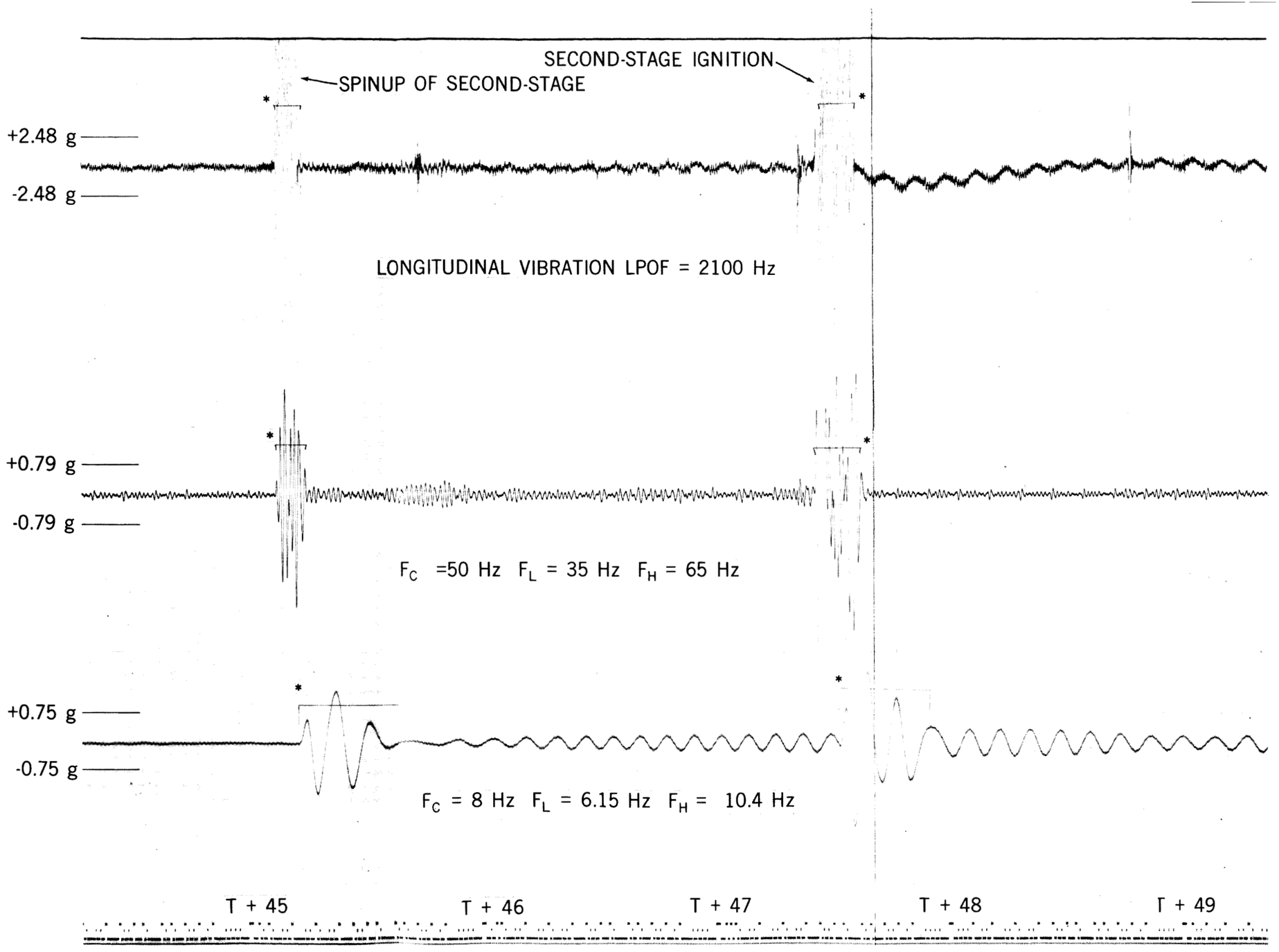

Figure 30. Longitudinal Vibration, T + 45.7 Sec : 50 and 8 Hz

PRECEDING PAGE BLANK NOT FILMED.

FOLDOUT FRAME

FOLDOUT FRAME

FOLDOUT FRAME

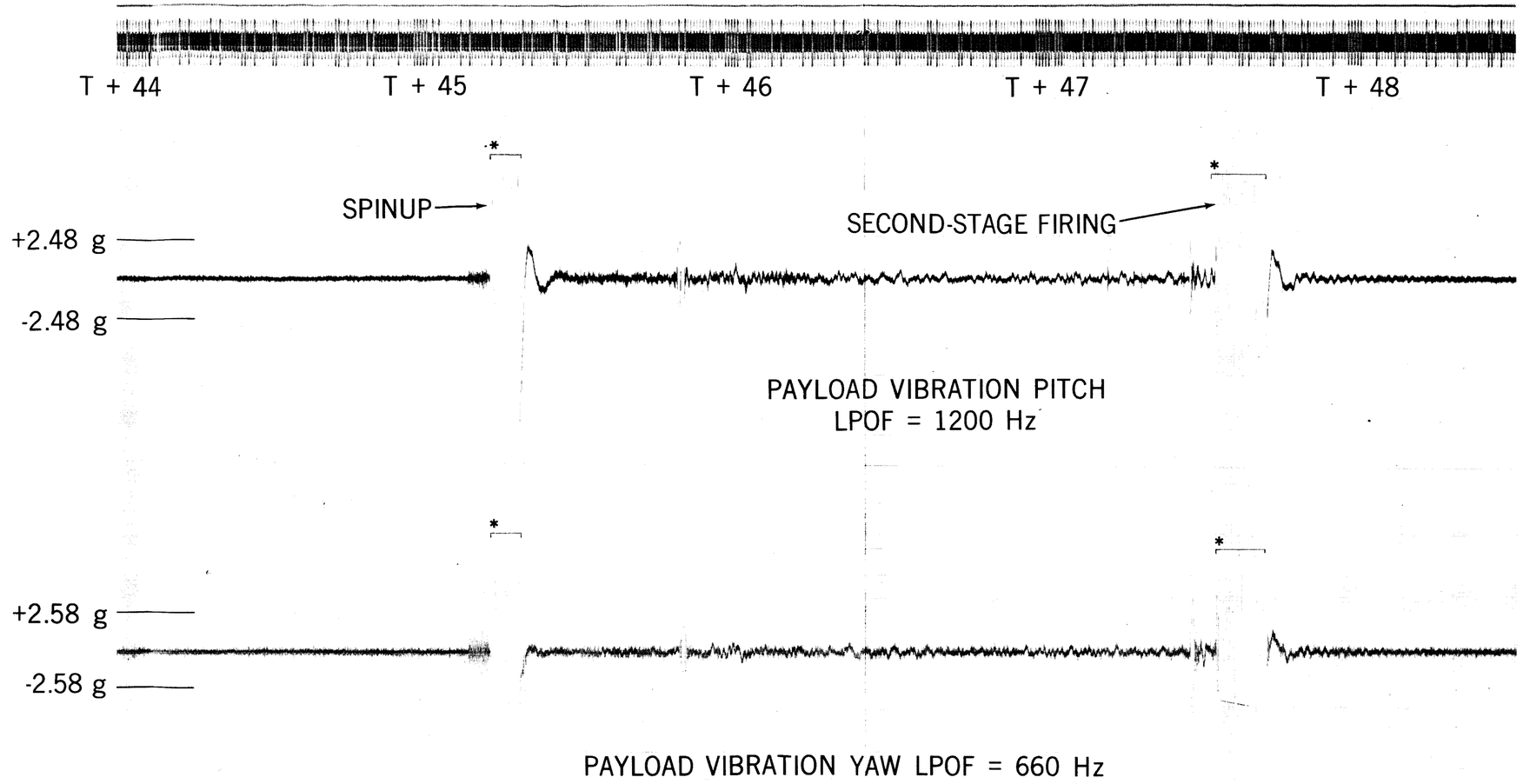

Figure 31. Pitch and Yaw Vibration, Second-Stage Events

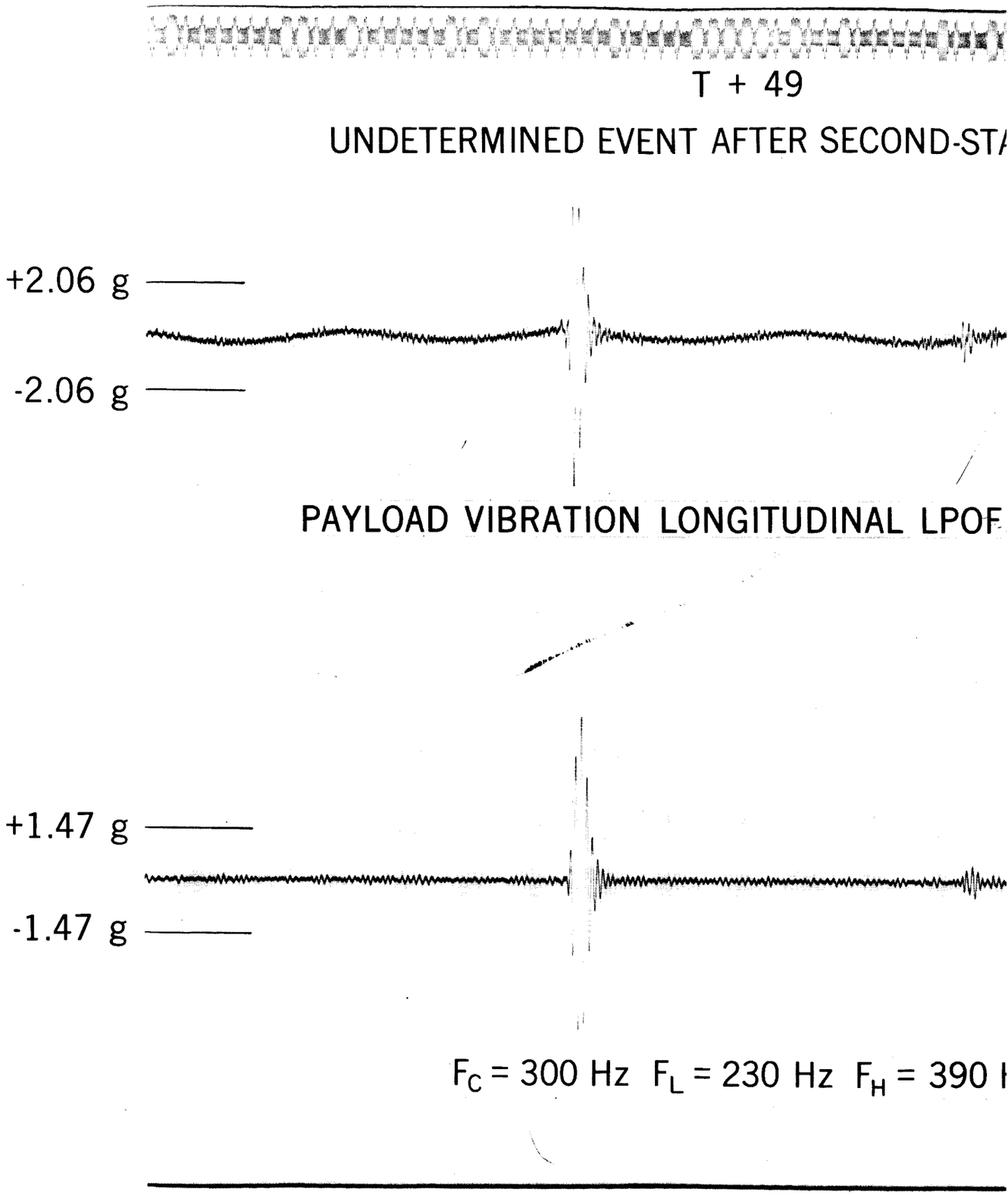

Figure 32. Longitudinal Vibration, Unidentified Impulse, T + 48.8 Sec : 300 Hz

FOLDOUT FRAME

FOLDOUT FRAME I

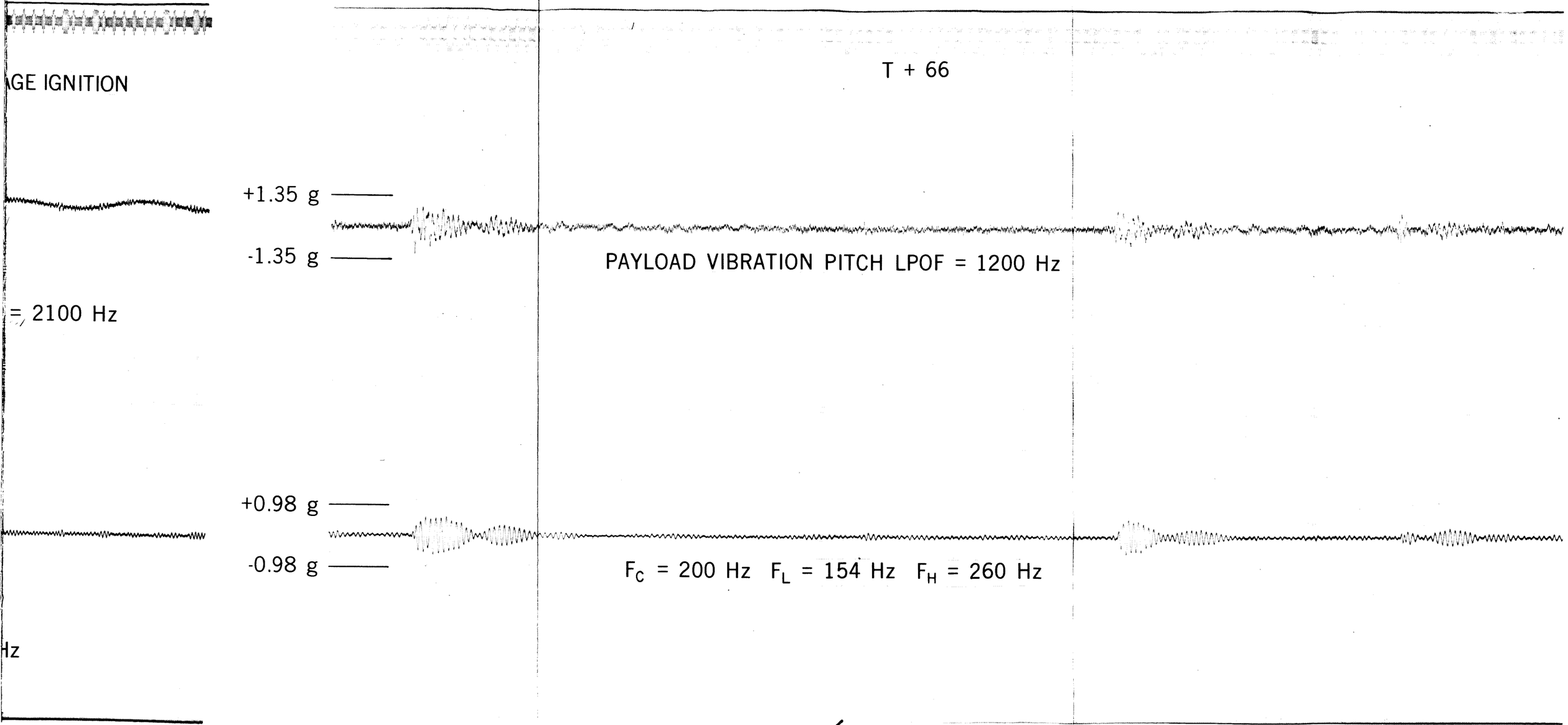

FOLDOUT FRAME II

FOLDOUT FRAME III

Figure 33. Pitch Vibration, Second-Stage Burn, T + 65.4 Sec : 200 Hz

FOLDOUT FRAME IV

T + 66

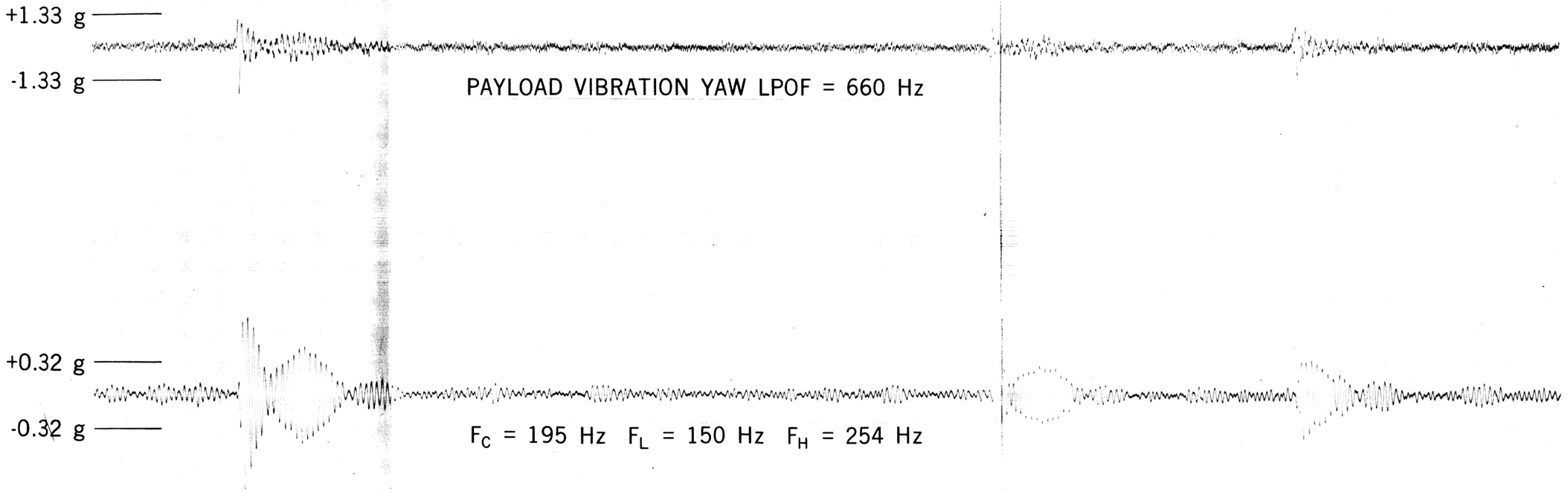

FOLDOUT FRAME 1

FOLDOUT FRAME 2

Figure 34. Yaw Vibration, Second-Stage Burn, T + 65.4 Sec : 200 Hz

FOLDOUT FRAME 3

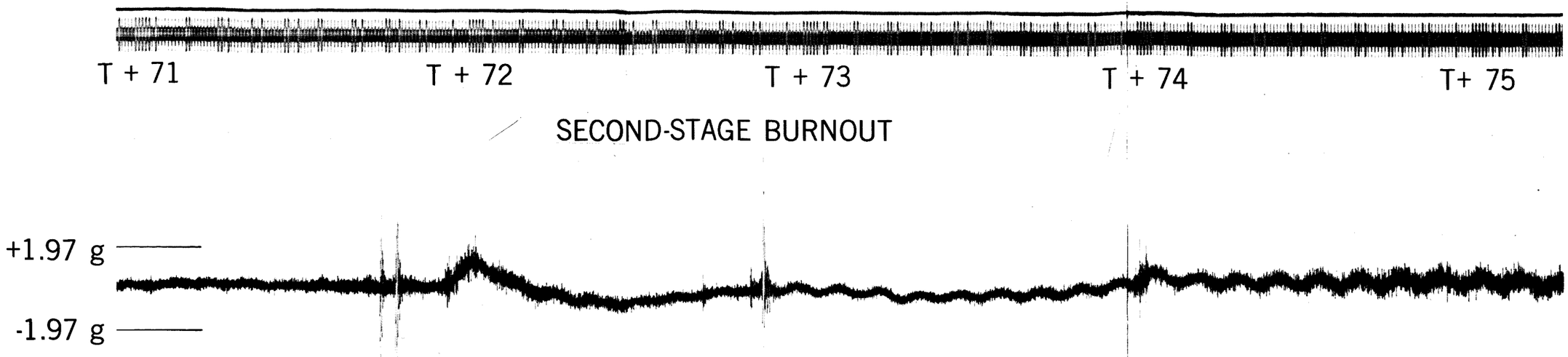

Figure 35. Longitudinal Vibration, Second-Stage Burnout, T + 75 Sec : 8 Hz

FOLDOUT FRAME I

FOLDOUT FRAME

FOLDOUT FRAME II

PRECEDING PAGE BLANK NOT FILMED.

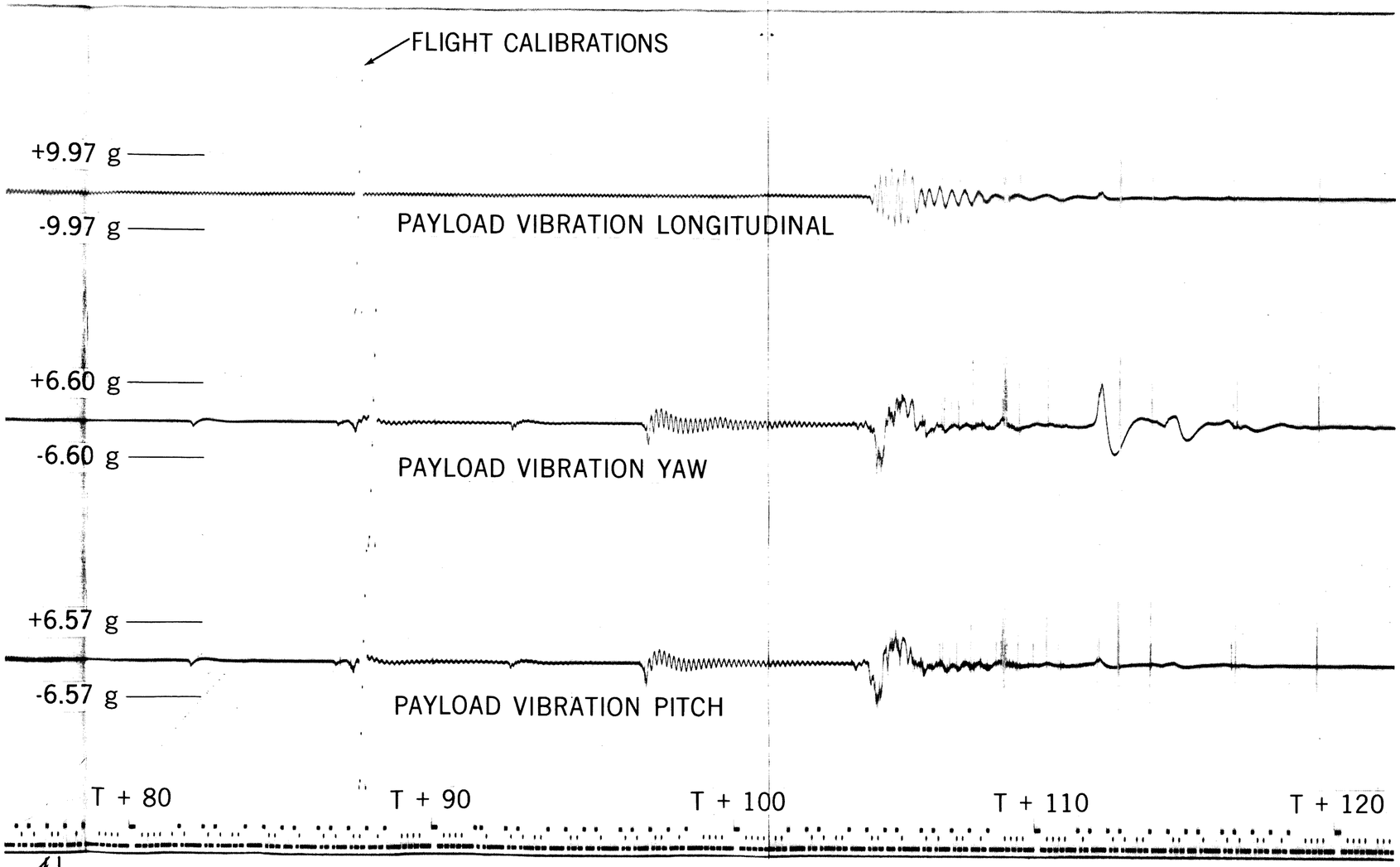

FOLDOUT FRAME #1

Figure 36. Erratic Vehicle Motions After Second-Stage Burnout

FOLDOUT FRAME #2

FOLDOUT FRAME

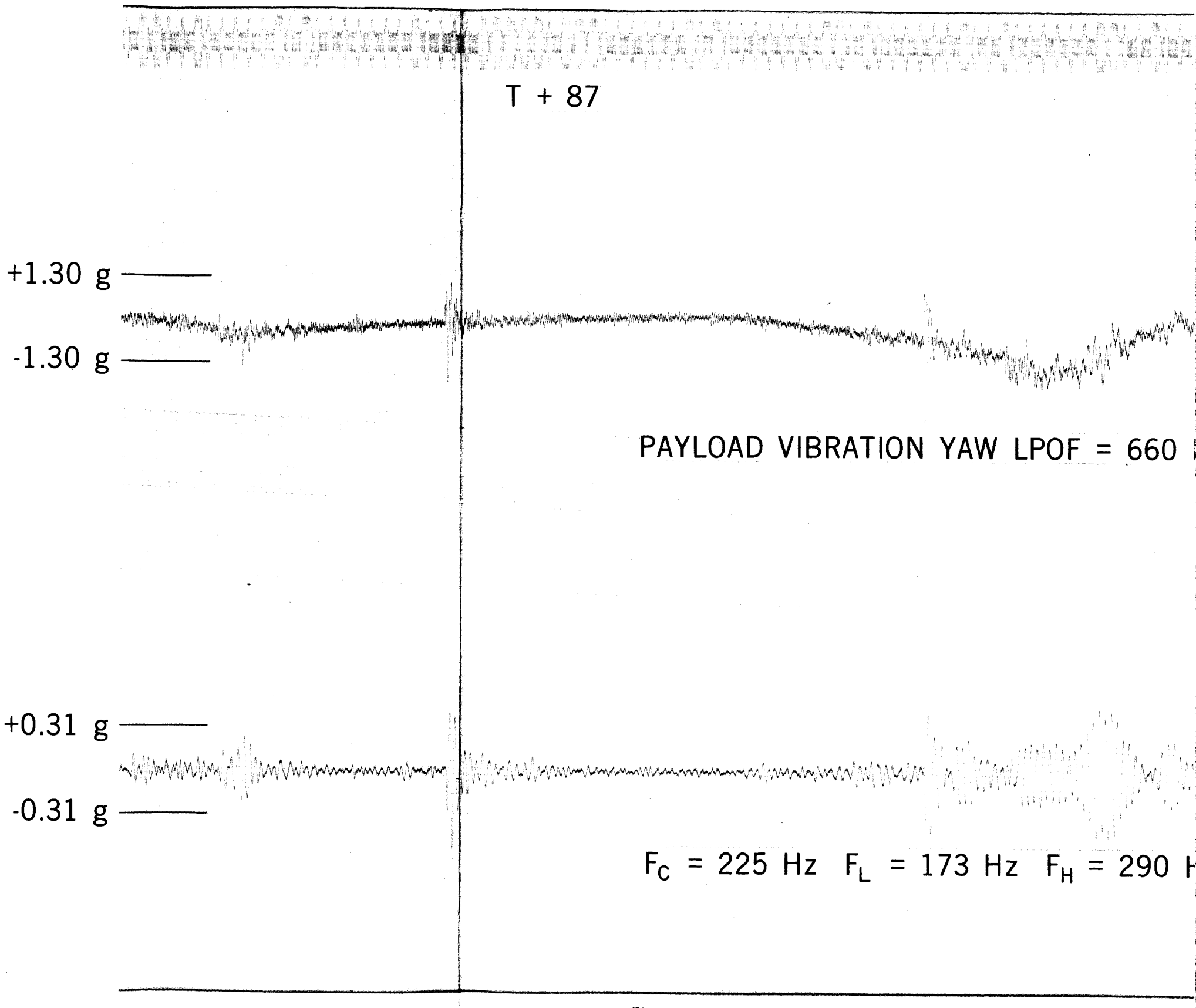

Figure 37. Yaw Vibration, Erratic Vehicle Motion, T + 87.4 Sec : 225 Hz

FOLDOUT FRAME 1

FOLDOUT FRAME 1

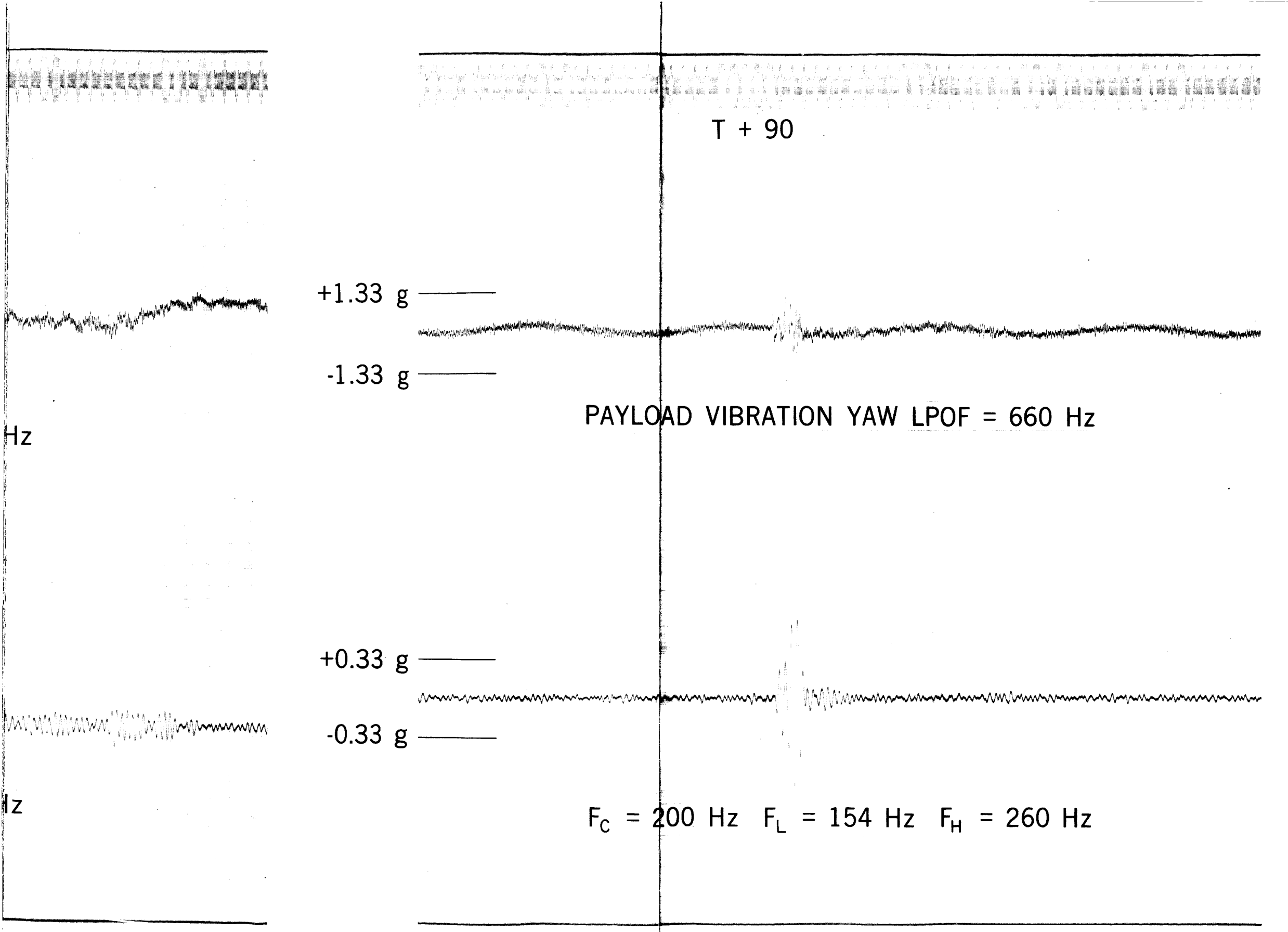

Figure 38. Yaw Vibration, Erratic Vehicle - Motion, T + 90 Sec : 225 Hz

FOLDOUT FRAME II

FOLDOUT FRAME 13

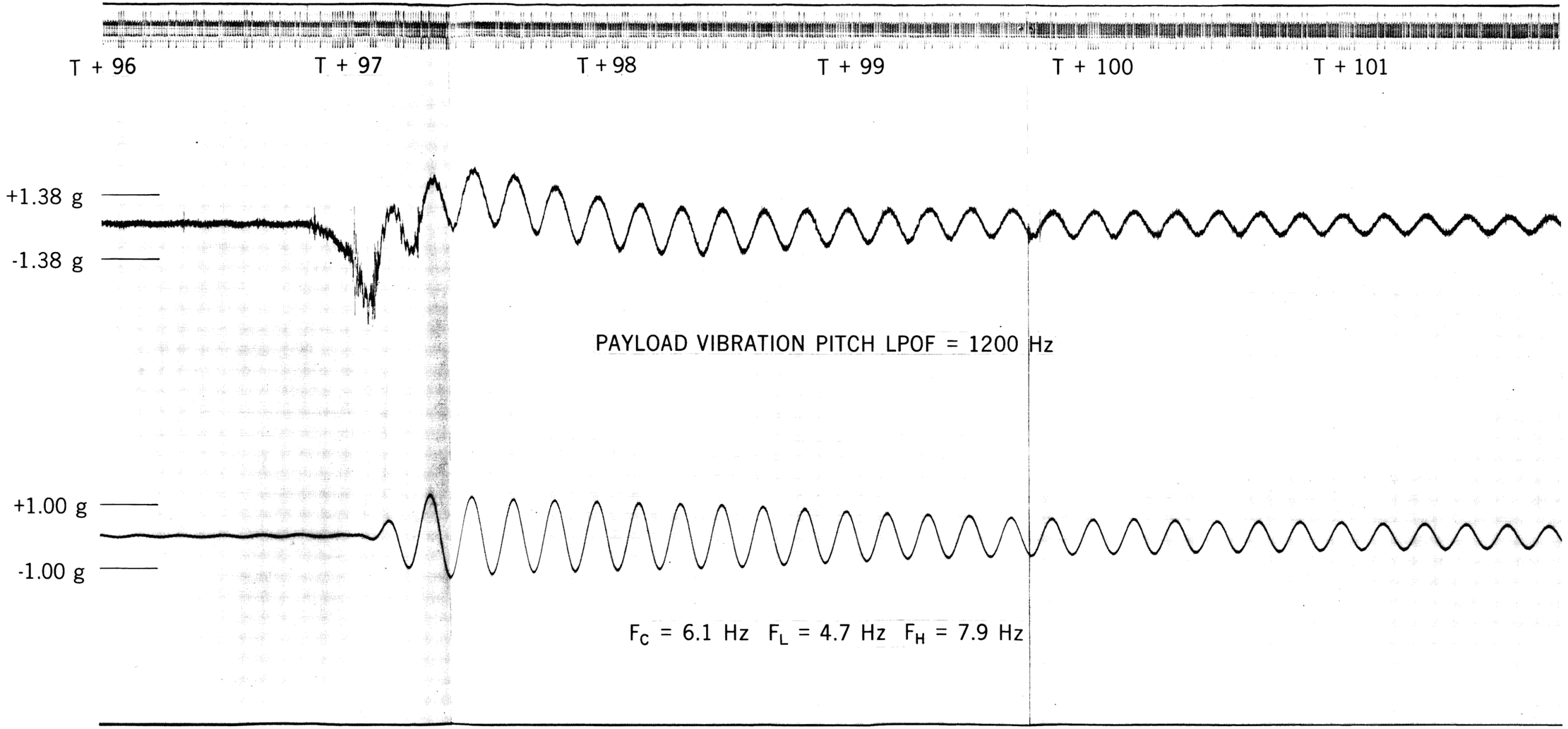

Figure 39. Pitch Vibration, Erratic Vehicle Motion, T + 97 Sec : 6 Hz

PRECEDING PAGE BLANK NOT FILMED.

FOLDOUT FRAME #1

FOLDOUT FRAME #2

FOLDOUT FRAME #3

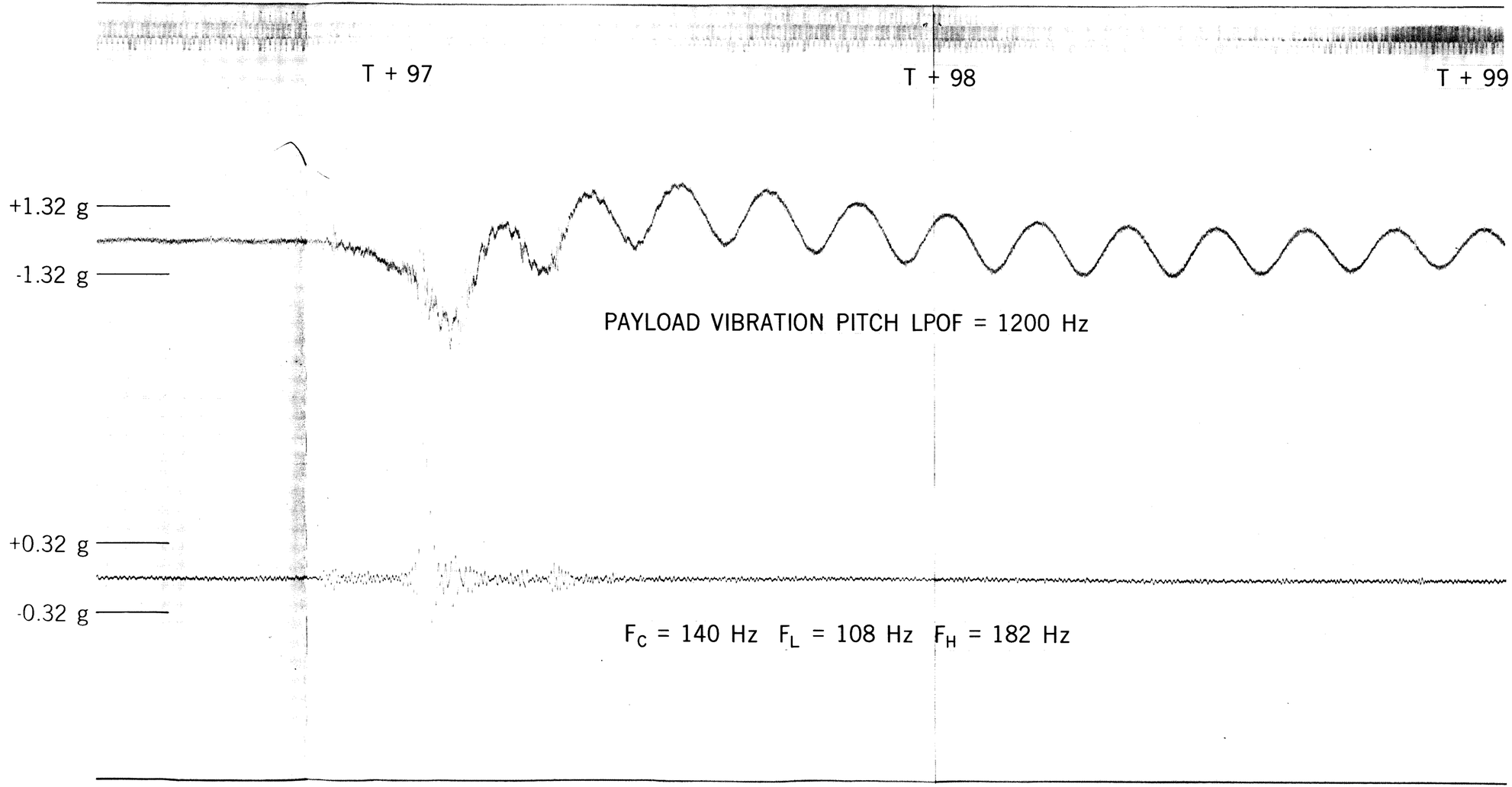

Figure 40. Pitch Vibration, Erratic Vehicle Motion, T + 97 Sec : 140 Hz

FOLDOUT FRAME #1

PRECEDING PAGE BLANK NOT FILMED.

FOLDOUT FRAME #2

FOLDOUT FRAME #3

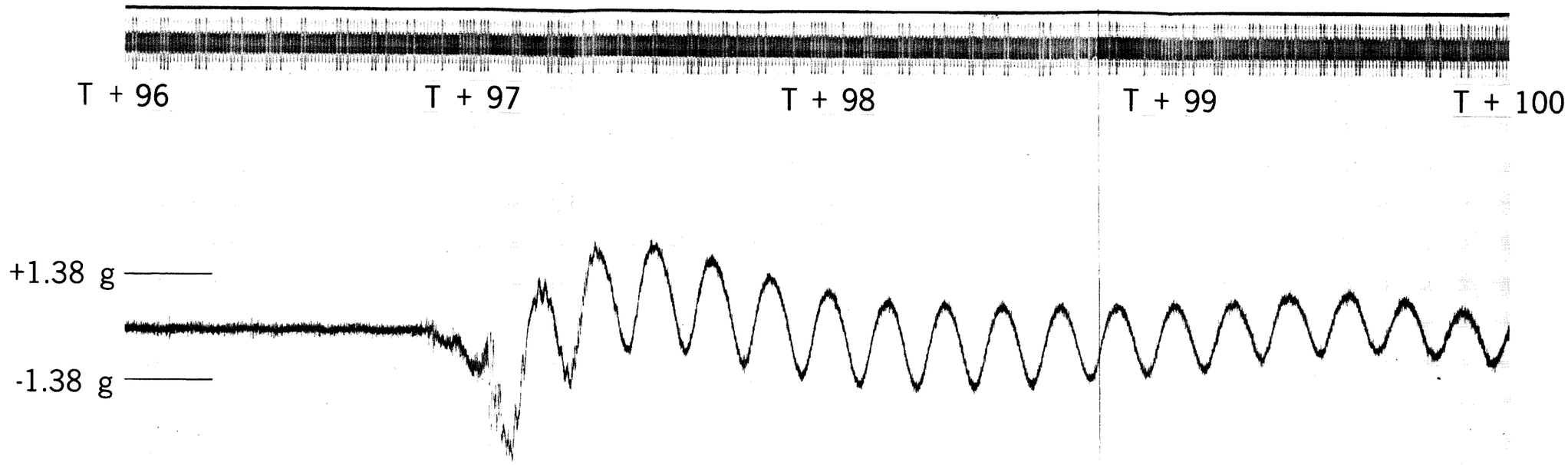

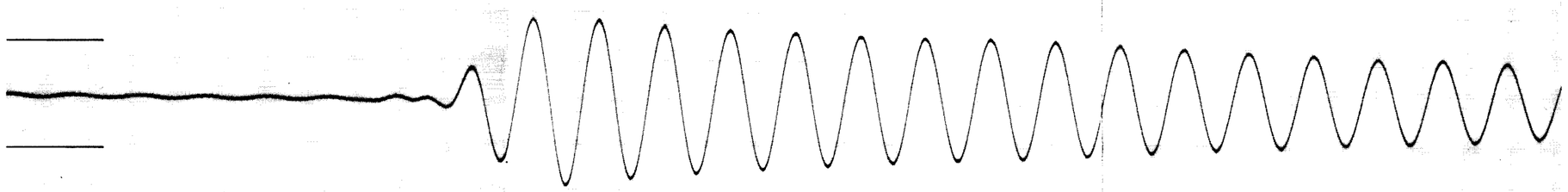

Figure 41. Yaw Vibration, Erratic Vehicle Motion, T + 97 Sec : 6 Hz

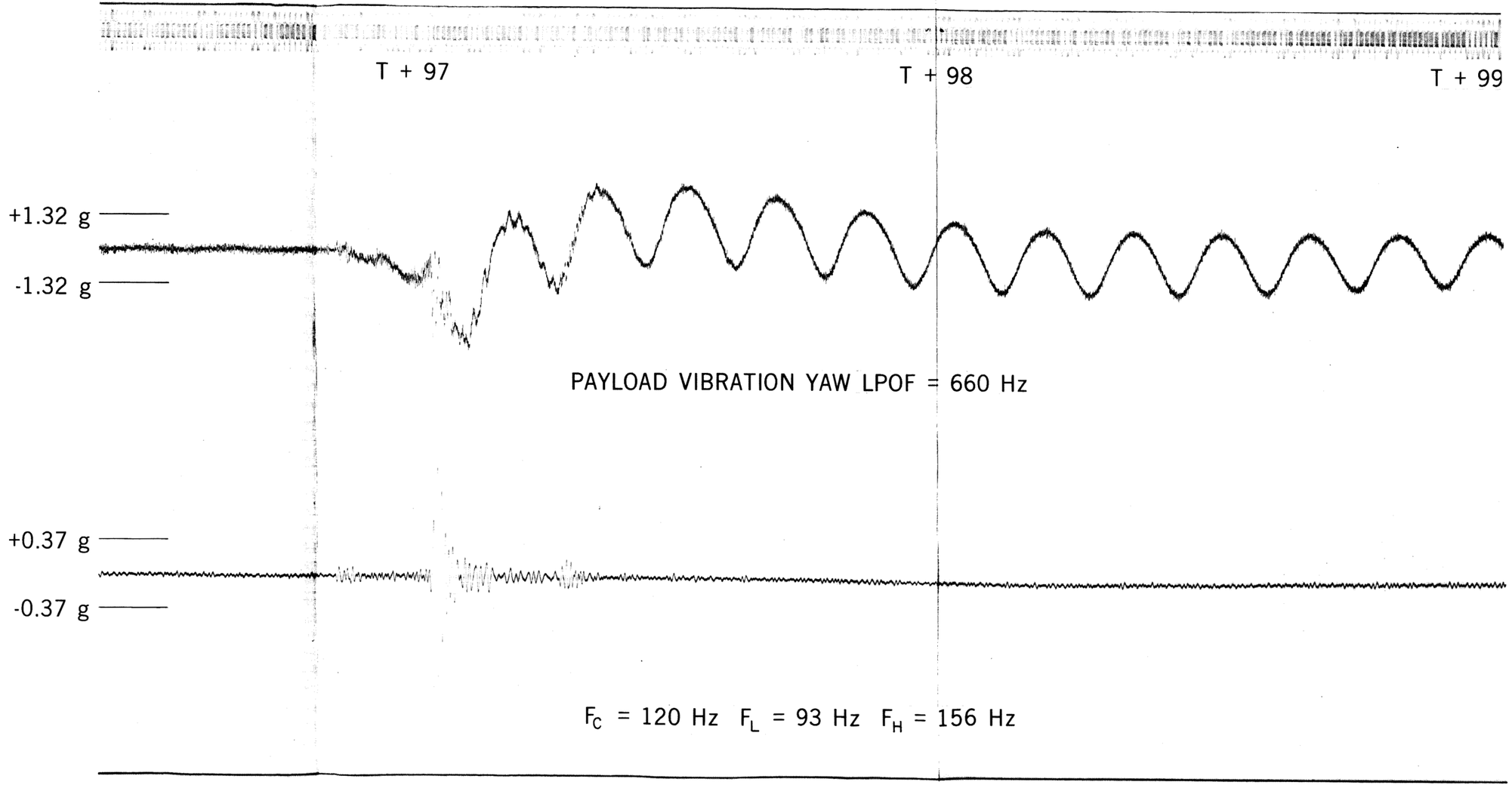

FOLDOUT FRAME #1

PRECEDING PAGE BLANK NOT FILMED.

FOLDOUT FRAME

FOLDOUT FRAME #2

Figure 42. Yaw Vibration, Erratic Vehicle Motion, T + 97 Sec : 140 Hz #3

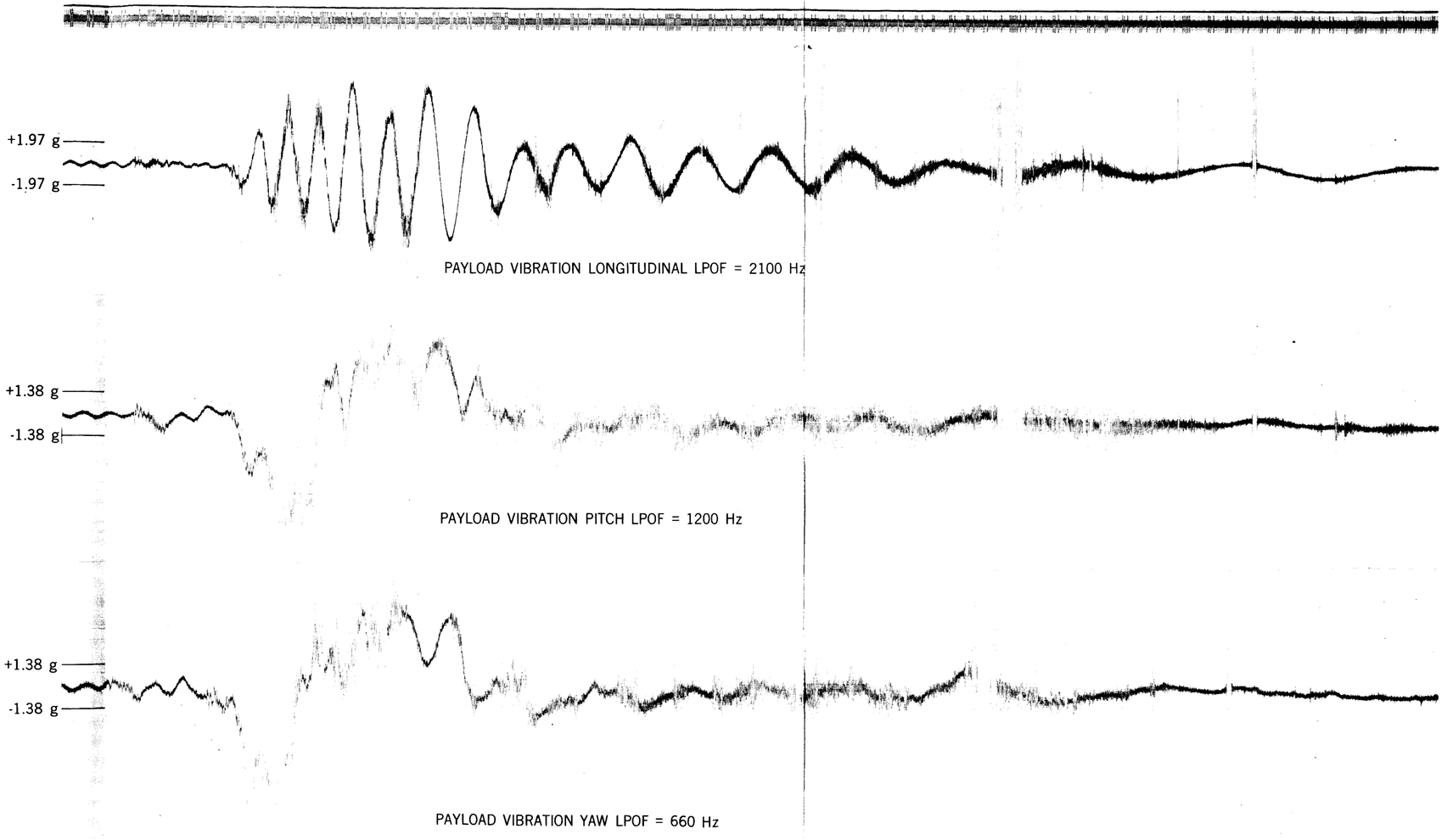

FOLDOUT FRAME #1

FOLDOUT FRAME

FOLDOUT FRAME 2

Figure 43. Longitudinal, Pitch, and Yaw Acceleration at T + 104 Sec Indicating Erratic Vehicle Motion

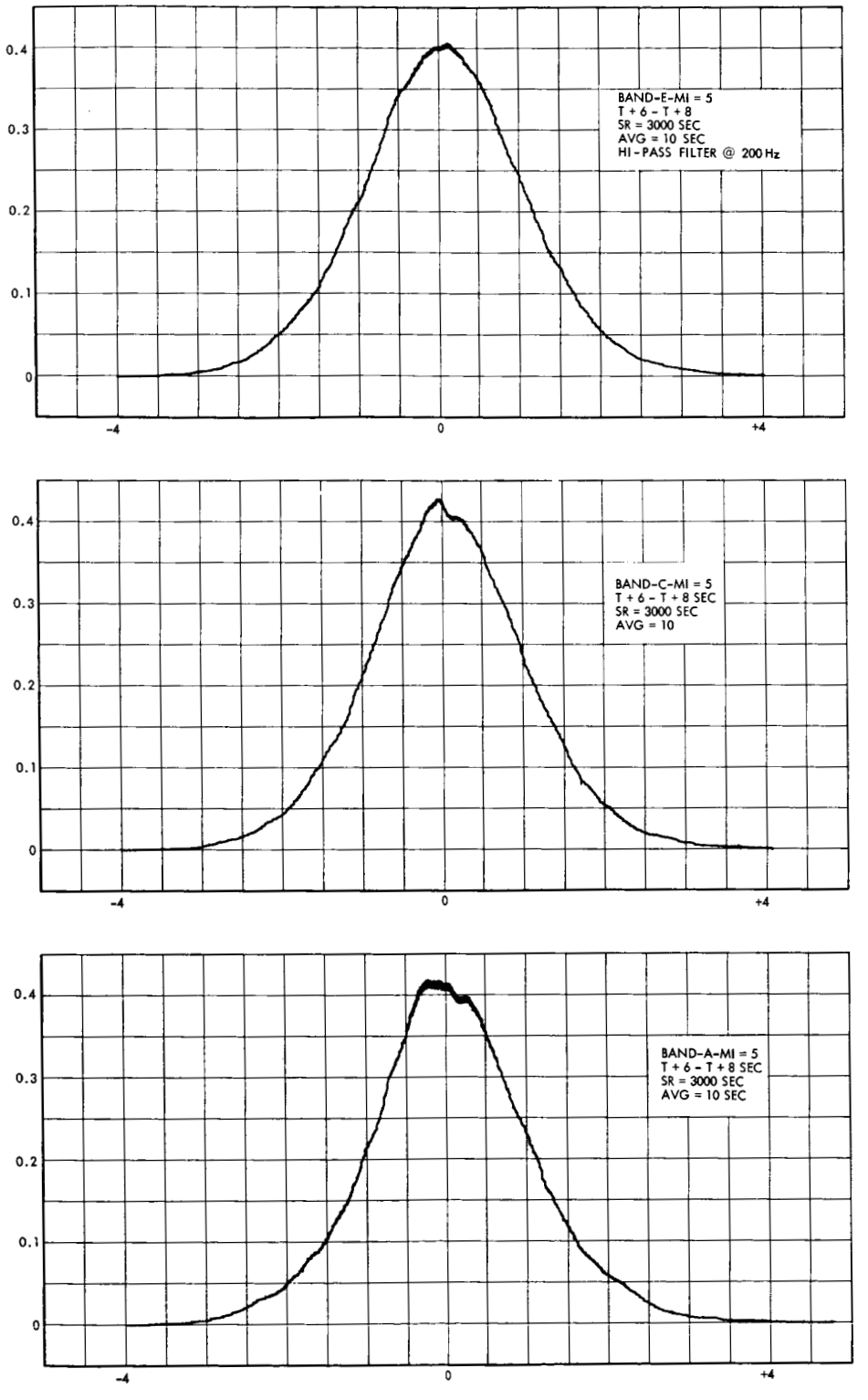

Figure 44. Probability Density Analysis, Longitudinal, Pitch, and Yaw Payload Vibration (T + 6 to T + 8 Sec)

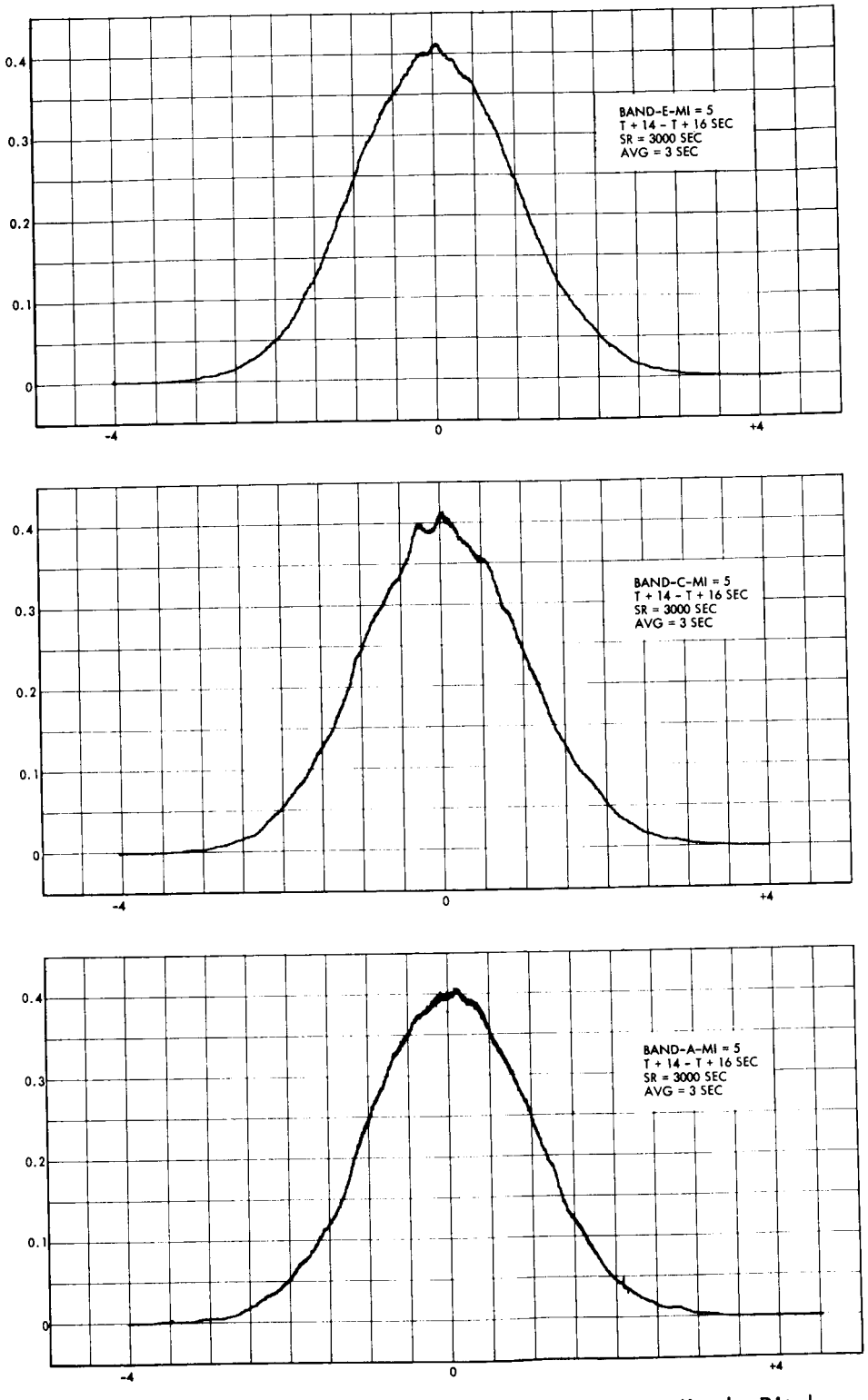

Figure 45. Probability Density Analysis, Longitudinal, Pitch, and Yaw Payload Vibration (T + 14 to T + 16 Sec)

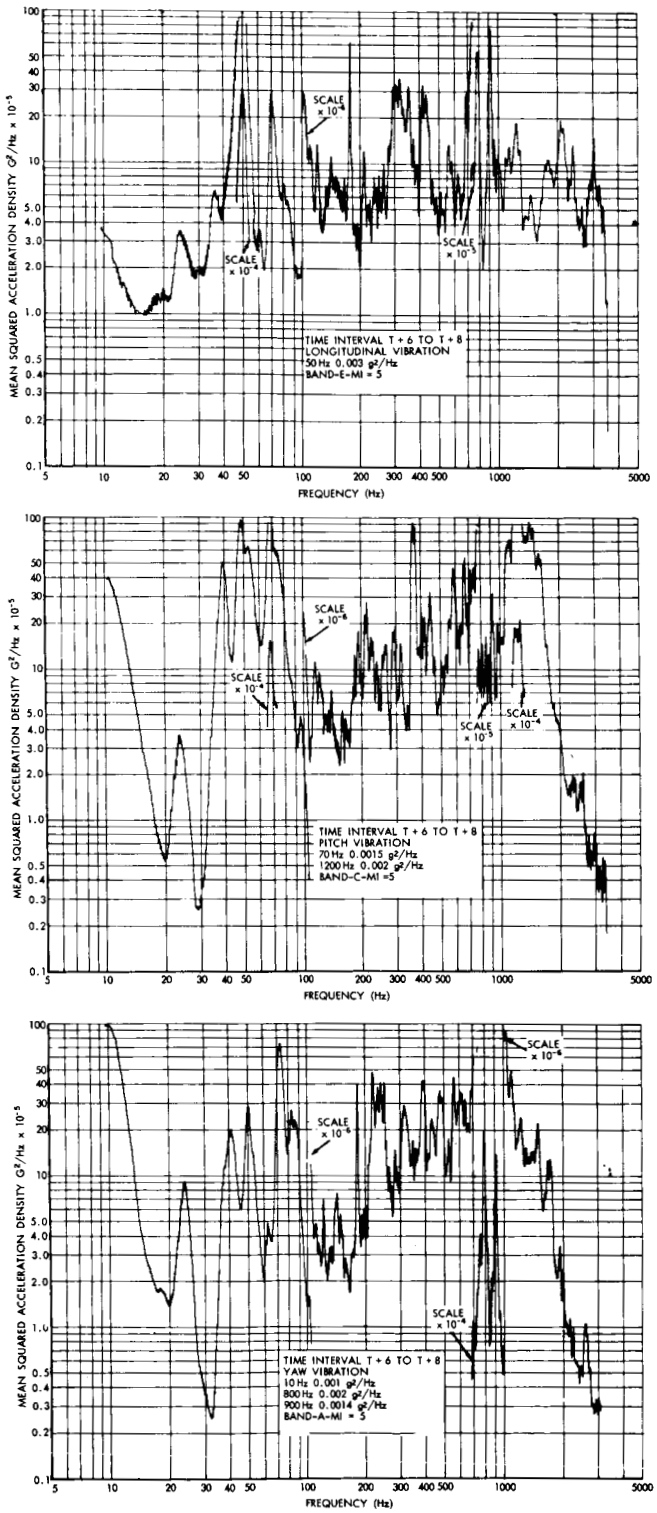

Figure 46. Power Spectral Density, Longitudinal, Pitch, and Yaw Payload Vibration (T + 6 to T + 8 Sec)

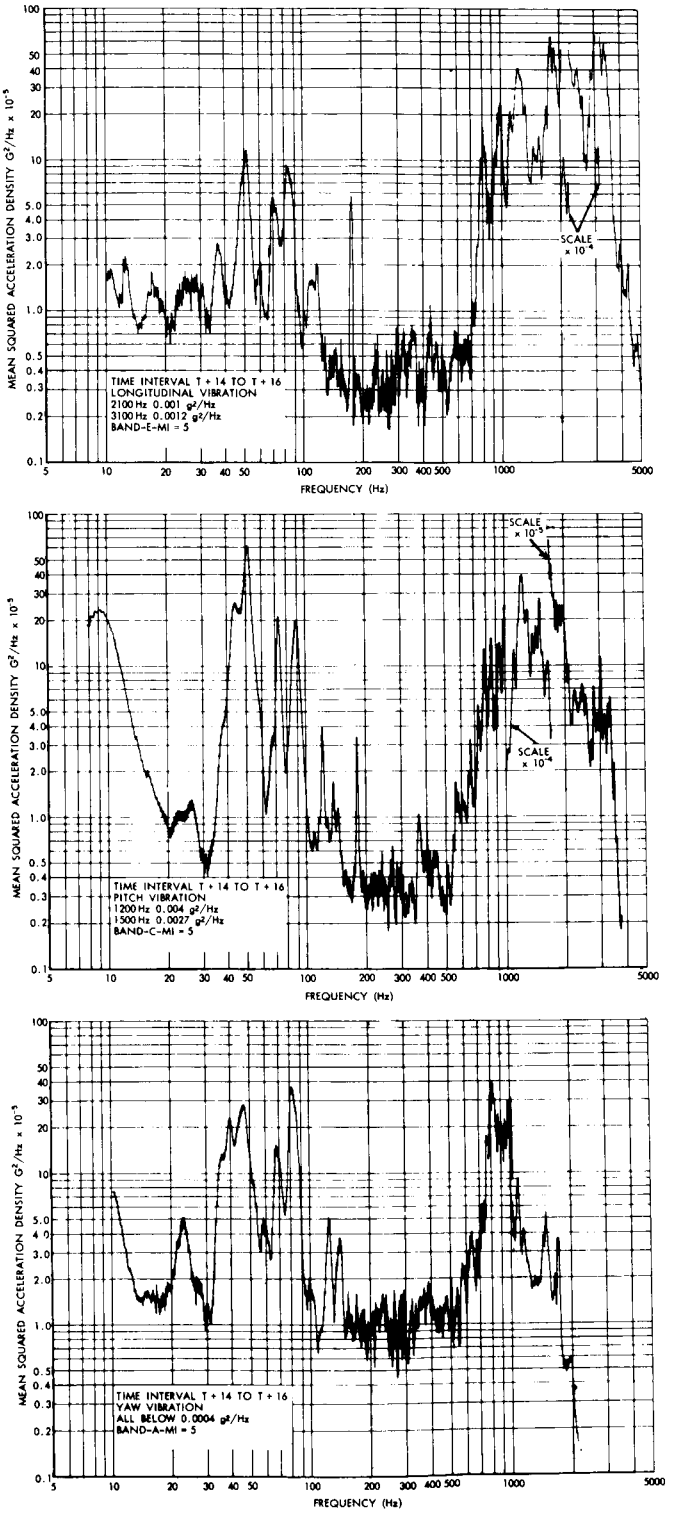

Figure 47. Power Spectral Density, Longitudinal, Pitch, and Yaw Payload Vibration (T + 14 to T + 16 Sec)

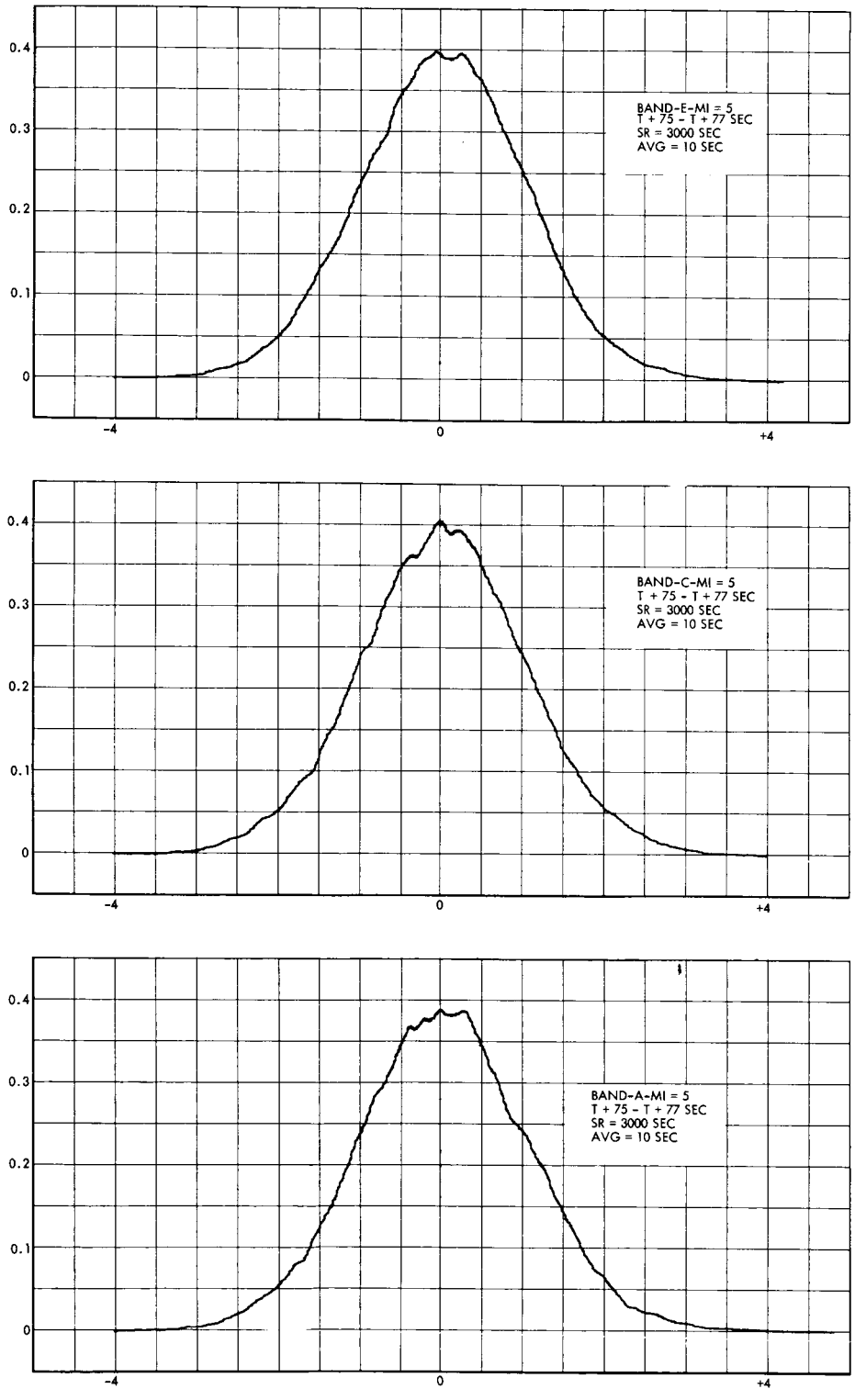

Figure 48. Probability Density Analysis, Longitudinal, Pitch, and Yaw Payload Vibration (T + 75 to T + 77 Sec)

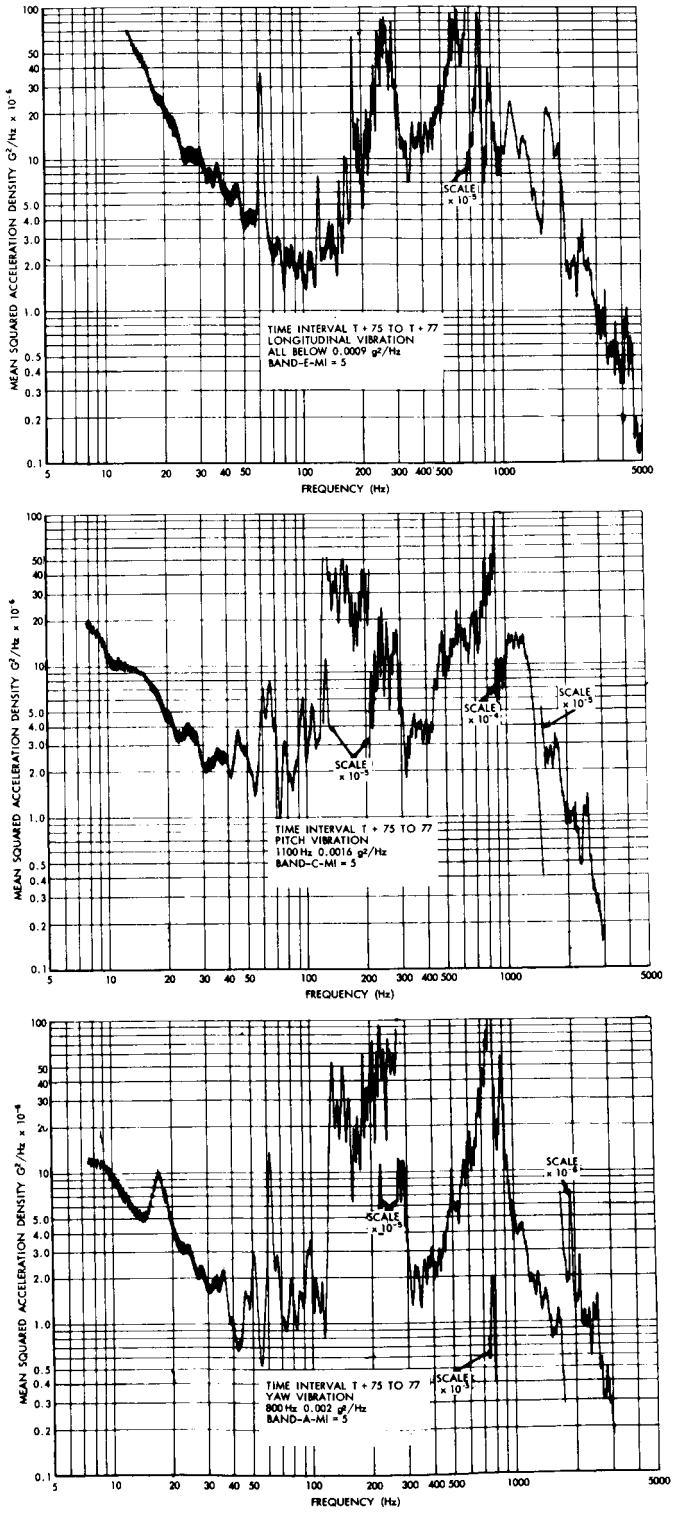

Figure 49. Power Spectral Density, Longitudinal, Pitch, and Yaw Payload Vibration (T + 75 to T + 77 Sec)